Multicriteria evaluation of the AquaCrop crop model in a hilly rainfed Mediterranean agrosystem

M. Dhouib (1), R. Zitouna-Chebbi (2), L. Prévot (3), J. Molénat (3), I. Mekki (2), F. Jacob (4)

(1) Institut Agro Montpellier/UMR LISAH, INRAE, IRD, Institut Agro Montpellier, AgroParisTech, University of Montpellier, Montpellier, France

(2) INRGREF, University of Carthage, Tunis, Tunisia

(3) INRAE/UMR LISAH, INRAE, IRD, Institut Agro Montpellier, AgroParisTech, University of Montpellier, Montpellier, France

(4) IRD/UMR LISAH, INRAE, IRD, Agro Montpellier Institute, AgroParisTech, University of Montpellier, Montpellier, France

Abstract

Exploring crop spatial organizations within landscapes is a promising solution for agroecological transitions and climate change adaptation in Mediterranean rainfed hilly agrosystems. A prerequisite is to ensure that crop models can simulate a range of agrohydrological processes in such agrosystems. The current study deepened the evaluation of the AquaCrop model by conducting a multicriteria evaluation (canopy cover CC, dry aboveground biomass AGB, actual evapotranspiration ET_a, runoff R, soil water content SWC) for a range of crop and soil combinations, and for contrasted hydroclimatic years in northeastern Tunisia. The data were collected in the Kamech catchment (OMERE Observatory) during nine measurement campaigns on predominant soils and crops. AquaCrop simulations were based on field observations and parameters from the literature.

AquaCrop could simulate plant dynamics and water fluxes for contrasted hydroclimatic years, with a slight dependence on soil class and a significant dependence on crop type. Model simulations were of moderate quality for CC (R^2 of 0.45, RMSE of 0.24 on average) and of acceptable quality for AGB (R^2 of 0.81, RMSE of 0.85 ton ha^{-1} on average). AquaCrop acceptably simulated water transfer across the soil–plant continuum (R^2 of 0.62, RMSE of 0.77 mm day^{-1} on average for ET_a; R^2 of 0.68, RMSE of 0.75 mm day^{-1} on average for R; R^2 of 0.86, RMSE of 27.4 mm on average for SWC). The model performances were satisfactory for most cases, with p values larger than 5% for the Student's t test on linear regressions of validation. Our results were similar to those reported in previous studies over flat terrain, including delayed senescence by model simulations with subsequent overestimation of CC and AGB observations. Additionally, soil cracks likely altered the AquaCrop ability to simulate runoff. Despite these limitations, our results support the application of AquaCrop to evaluate water productivity in hilly agrosystems.

Keywords

AquaCrop model; Rainfed agrosystems; Hilly terrains; Multicriteria evaluation; Mediterranean soils and crops; Soil water balance

1. Introduction

Mediterranean agriculture is an important sector from economic, social and environmental perspectives, especially for the southern and eastern Mediterranean countries. It is a significant contributor to gross domestic product (GDP) in these countries; it ensures food security, and it helps reduce rural migration by providing local jobs (Tanyeri-Abur, 2015). Rainfed agriculture covers 80% and 75% of cultivated lands in the world and North Africa, respectively (Bhattacharya, 2019; Wani et al., 2009). It is generally based on family systems, and it has significant room for improvement in water productivity (Ruben and Pender, 2004). In hilly areas, the productivity of rainfed agriculture depends not only on the rainfall regime but also on the spatiotemporal distribution of surface water and sediment flows (Norouzi et al., 2010). Until now, Mediterranean public policies within hilly areas have mainly focused on mobilizing blue water resources for irrigated agriculture through the planning of hydroagricultural infrastructures (e.g., dams, reservoirs) and have focused less on optimizing the use of green water for rainfed agriculture (Nouri et al., 2020).

Despite of numerous benefits for Mediterranean hilly areas, rainfed agriculture undergoes several pressures (Brun et al., 2016), either climate-driven (floods and erosion, heat waves, rainfall shortages) or anthropogenic-driven (population growth, increasing agricultural activities and hydroagricultural infrastructures). From a sustainability perspective, it is important to quantitatively manage agricultural water, where some of the numerous solutions to be explored involve the spatiotemporal modulation of anthropogenic actions, individually or in combination (IAASTD, 2008). These solutions imply processes (fluxes, storages and transformations) and several components (e.g., root zone, aquifer, vegetation, hydroagricultural infrastructures, agricultural practices) within agrosystems. The exploration of these solutions must account for two key points. First, in situ scientific experiments are not suitable for both large agricultural areas and forecasts in a climate change context, which makes necessary the use of process modelling for numerical simulations (Jones et al., 2017). Second, the water cycle and crop dynamics are strongly linked. Vegetation cover drives the rainfall repartition between runoff and infiltration in relation to fluxes within hydrographic networks towards lakes and reservoirs, to soil water storage and to aquifer refill. The water cycle drives root zone water content and crop water consumption, with consequences on agricultural yields. It is therefore important to properly characterize the interactions between the water cycle and crop functioning within agrosystems (Kanda et al., 2018).

Integrated process modelling should be able to simulate, within hilly catchments, crop functioning and the water cycle along with their interactions. This requires parsimonious crop models that (1) minimize the number of parameters for realistic simulations with spatialization purposes and (2) simulate crop functioning in relation to water dynamics within the root zone layer and underlying shallow aquifer. The literature provides a large number of crop models that describe plant functioning and growth along with crop yield (Weiss et al., 2020). Well known examples are APSIM (Keating et al., 2003), DSSAT (Jones et al., 2003), EPIC (Williams et al., 1984), STICS (Brisson et al., 2003), WOFOST (Todorovic et al., 2009; de Wit et al., 2019), AquaCrop (Raes et al., 2009; Steduto et al., 2009), CropSyst (Stöckle et al., 2003), or AqYield (Constantin et al., 2015; Tribouillois et al., 2018). Based on the primary factors that describe crop functioning, Todorovic et al. (2009) classified crop models into (1) carbon-driven models such as WOFOST, CROPGRO, and DSSAT, (2) solar radiation-driven models such as CERES, EPIC, STICS, and APSIM, and (3) water-driven models such as AquaCrop and CropSyst in which biomass production is proportional to the amount of transpired water. CropSyst is a model based on water and solar radiation. When the vapour pressure deficit (VPD) is very low, the transpiration-biomass relationship is replaced by a radiative approach in which biomass is determined on the basis of intercepted photosynthetically active radiation

(IPAR, Stöckle et al., 2003; Kanda et al., 2018). Among the aforementioned crop models, AquaCrop is therefore the unique water-driven model (Kanda et al., 2018). It is thus an interesting model for addressing the coupling of crop functioning and the water cycle within Mediterranean hilly catchments typified by rainfed agriculture. In addition, it provides a trade-off between robustness and simplicity, since it requires a moderate number of input parameters.

The literature includes numerous studies that involve AquaCrop. These studies can be classified into four main groups, according to their content: (1) calibration, validation, and performance evaluation of the model in specific contexts (Mkhabela and Bullock, 2012; Zeleke, 2019); (2) cropping system management on the basis of model simulations: estimation of crop water requirements, sowing dates and crop yields, as well as consequences of fertilization, salinity, and irrigation regimes on crop yield (Araya et al., 2010; Qin et al., 2013; Nyakudya and Stroosnijder, 2014; El Mokh et al., 2017; Er-Raki et al., 2021); (3) impact of climate change on crop production and evaluation of different adaptation strategies (Muluneh, 2020; Raoufi and Soufizadeh, 2020; Rashid et al., 2019); and (4) economic impact of cropping practices and climate change on productivity (Cusicanqui et al., 2013; Bird et al., 2016). Meanwhile, AquaCrop has been used across the five continents, under different climates (Mediterranean, tropical, continental, temperate) and within both irrigated and rainfed agrosystems (Geerts et al., 2009; García-Vila and Fereres, 2012; García-López et al., 2014; Vanuytrecht et al., 2014; Ahmadi et al., 2015; Deb et al., 2015; Shrestha et al., 2016; Silvestro et al., 2017; Xing et al., 2017; Sandhu and Irmak, 2019; Lu et al., 2021). Overall, AquaCrop has been tested and validated on a wide range of agroenvironmental conditions.

Some of the aforementioned AquaCrop-based studies focused on variables describing crop growth, such as canopy cover CC, dry aboveground biomass AGB and yield (Todorovic et al., 2009; Mkhabela and Bullock, 2012; Silvestro et al., 2017). Other studies addressed actual evapotranspiration (ET_a) (Geerts et al., 2009; Katerji et al., 2013) as well as soil water content

(SWC) (Nyakudya and Stroosnijder, 2014; Sghaier et al., 2014). Similar to most crop models, AquaCrop was designed and evaluated for local applications at the plot level over flat terrains. More recently, the model was evaluated on hilly terrains, either in a multilocal way that disregarded interplot water exchanges (Alaya et al., 2019; Han et al., 2019) or in a distributed way that accounted for interplot water exchanges (Van Loo and Verstraeten, 2021). However, more research is needed to address the diversity of situations induced by Mediterranean rainfed hilly agrosystems in relation to cropping, soil and topographic conditions. In addition, AquaCrop was evaluated on only a few variables simultaneously, whereas any multicriteria evaluation is likely to provide a better assessment of model capacities.

The objective of this study is to deepen the evaluation of the capabilities of the AquaCrop model for rainfed crops within hilly Mediterranean catchments. We propose (1) to consider little-studied crops (e.g., faba bean and oats) under subhumid to semiarid climates, (2) to consider combinations of crops (faba bean, oats, wheat, barley) and soils (Vertisols, Cambisols and Luvisols) for contrasted hydroclimatic years, and (3) to conduct a more substantial multicriteria analysis that includes simultaneously vegetation canopy (CC, AGB), soil water content integrated over topsoil and root zones, and water fluxes (ET_a, runoff as infiltration excess). We focus here on the evaluation of AquaCrop without addressing calibration issues. The current paper is structured as follows. We briefly present the AquaCrop model. We introduce the study area and the datasets used, as well as the strategy for evaluating the model. Thereafter, we analyse the comparison of the simulations against the observations by exploring the possible influences of soil and crop type. We finally discuss these results in light of former studies, and we conclude with our contribution to the assessment of AquaCrop performances, along with further perspectives.

2. Presentation of the AquaCrop model

Detailed presentations of AquaCrop (https://www.fao.org/aquacrop/en/) are given by Steduto et al., (2009), Raes et al. (2009) and Salman et al. (2021). We detail here the specificities related to the methodological choices on which the current study relies. Developed by FAO, AquaCrop is a parsimonious (reduced number of parameters) crop model that aims to simulate crop biomass and yield by considering water as the main driver of crop functioning (Kanda et al., 2018). Operating at a daily time step, AquaCrop simulates the vertical exchanges between the different components of the soil–plant-atmosphere continuum.

AquaCrop describes the soil as a reservoir split into several horizons (5 maximum). Each horizon is characterized by texture or related hydrodynamic properties: soil moisture at field capacity (HFC), soil moisture at wilting point (HWP), soil moisture at saturation (HSAT), saturated hydraulic conductivity (KSAT) and drainage coefficient (τ).

The model calculates soil evaporation (Es) and crop transpiration (Tr) separately, which permits the quantification of the amount of water unused by vegetation (Steduto et al., 2009). Another feature of the model is the description of canopy growth by using canopy cover (CC) instead of leaf area index (LAI). The model calculates Tr as a function of CC, and biomass is determined as a function of both Tr and normalized water productivity (WP*). The yield is finally calculated by multiplying biomass by harvest index (HI). Water productivity (WP*) accounts for atmospheric concentration [CO_2] and therefore permit to apply AquaCrop in prospective climate contexts related to precipitation, air temperature, evaporative demand and [CO_2].

The soil water content at each time step results from the balance of drainage, infiltration from rainfall/irrigation, soil evaporation and crop transpiration. AquaCrop accounts for four types of stress that affect crop growth: water stress, heat stress, fertilization stress and salinity stress.

Depending on the type of stress, the target parameters of the model change. For example, water stress affects leaf and CC expansion, root zone expansion, transpiration and the harvest index.

The main variables simulated by the model relate to crop productivity (canopy cover, dry aboveground biomass and yield) and water balance (soil water content, runoff, infiltration, drainage, capillary rise, soil evaporation and vegetation transpiration). The model parameters are related to the crop (conservative parameters, fixed for a given species and nonconservative parameters, varying according to the varieties), the soil (horizon number, texture or hydrodynamic parameters), and the groundwater table (depth). The forcing variables of the model are the climatic variables: reference evapotranspiration (ET_0), air temperature, rainfall and mean annual [CO2]. Agricultural practices include sowing date, fertilization and irrigation. Finally, the initial conditions include the initial soil water and salinity content.

3. Materials and methods

3.1. Study site

The study was conducted within the Kamech catchment, which is the southern site of the Mediterranean Observatory of Rural Environment and Water (French acronym OMERE, Molénat et al., 2018) that has collected multiple observations over the last 30 years. Kamech is a small hilly catchment area (2.6 km² size) located within the Cap-Bon Peninsula, northeastern Tunisia (10°52'-10°53'E and 36°52'-36°53' N, 108 m above sea level - asl.). It is representative of the climatic and cropping conditions of the region. The climate is Mediterranean subhumid/semi-arid. The rainy season spans from October to March (Mekki, 2003) with a cumulative rainfall of 635 mm (annual average over the [1994-2020] period) and an annual reference evapotranspiration of 1366 mm (Molénat et al., 2018). The area is 70% agricultural, combining crops and livestock, with significant spatiotemporal variability in land cover and spatial heterogeneity in soil types (Mekki, 2003; Mekki et al., 2006).

The Kamech catchment is typified by a diversified land cover that encompasses rainfed and fodder crops (Mekki, 2003; Zitouna-Chebbi et al., 2018). The dominant crops are winter cereals (durum wheat, barley, oats and triticale) and legumes (chickpeas, faba bean and peas). Altitudes range from 80 m to 200 m, and terrain slopes vary between 0 and 30%. The geological substratum is from the Miocene epoch, and it is mainly made of marl and clay (Mekki, 2003; Molénat et al., 2018). The four dominant soils are Cambisols, Luvisols, Vertisols and Regosols. They cover 46%, 26%, 10% and 18% of the catchment area, respectively (Mekki et al., 2018b). The soil depth varies from a few millimetres to 2 m.

Kamech is also typified by a large occurrence of swelling clay soils with shrinkage cracks that occur from March to December (Mekki, 2003; Inoubli, 2016). The closing of cracks heavily depends on rainfall at the beginning of the wet season and completely ends after cumulative rainfalls of approximately 200 mm ± 50 mm (Mekki, 2003). At their maximum opening, they have a water storage capacity of approximately 70 mm. Runoff occurs from December to March, when cracks are closed (Mekki, 2003; Inoubli, 2016).

3.2. Datasets

The current study benefits from a large database collected over the last three decades in the framework of the OMERE Observatory. This database includes meteorological, pedological, hydrological and agronomic observations (Mekki et al., 2006, 2018; Zitouna-Chebbi et al., 2018; Inoubli et al., 2017). This permitted to perform a thorough, multicriteria evaluation of the AquaCrop model.

We chose wheat/barley, oats and faba bean as representative species of grain cereals, fodder cereals and legumes, respectively. For each of these crops, some datasets were available between 2001 and 2013. Each of these datasets included a range of observations collected throughout a crop cycle on a given plot from September to August that also corresponded to a hydrological year. We selected the nine most complete datasets for conducting the AquaCrop multicriteria evaluation. This resulted in the combination of five years and eight plots. Table 1 shows the available datasets, including the panel of data available in each of the nine datasets for the AquaCrop multicriteria evaluation. Fig. 1 shows the location of the plots within the Kamech catchment. In the panel of plots presented in Fig. 1, plot A differs from the others. Indeed, this plot has been dedicated for two decades to regular monitoring as part of the OMERE Observatory. This monitoring included meteorological forcing, surface and subsurface hydrological monitoring, vegetation monitoring and soil characterization.

In the remainder of this section, we present the climatic, pedological, agronomic and hydrological data, by distinguishing between (1) the data used as inputs to the AquaCrop model and (2) the data used for the multicriteria evaluation of the model simulations.

__Table 1.__ The nine available datasets for the multicriteria evaluation of AquaCrop. LAI_plan, CC_visu, ET_a, *R and SWC stand for LAI from planimetric measurements, canopy cover from visual quantification, actual evapotranspiration, runoff and soil water content, respectively. The value Y of the label Year is related to harvesting year, and thus corresponds the crop cycle that spreads from September of year Y-1 to August of year Y.*

Crop	**Dataset**		**Available data**					
	Year	**Plot**	**LAI_plan**	**CC_visu**	ET_a	**R**	**SWC**	**AGB**
Wheat	2001	P7	x			x	x	x
	2002	P9	x			x	x	x
	2013	A	x		x	x	x	x
Barley	2006	D	x				x	
Oats	2002	P6	x			x	x	x
	2005	B	x		x		x	x
Faba	2001	P5		x		x	x	x
	2001	P8		x		x	x	x
	2002	P7		x		x	x	x

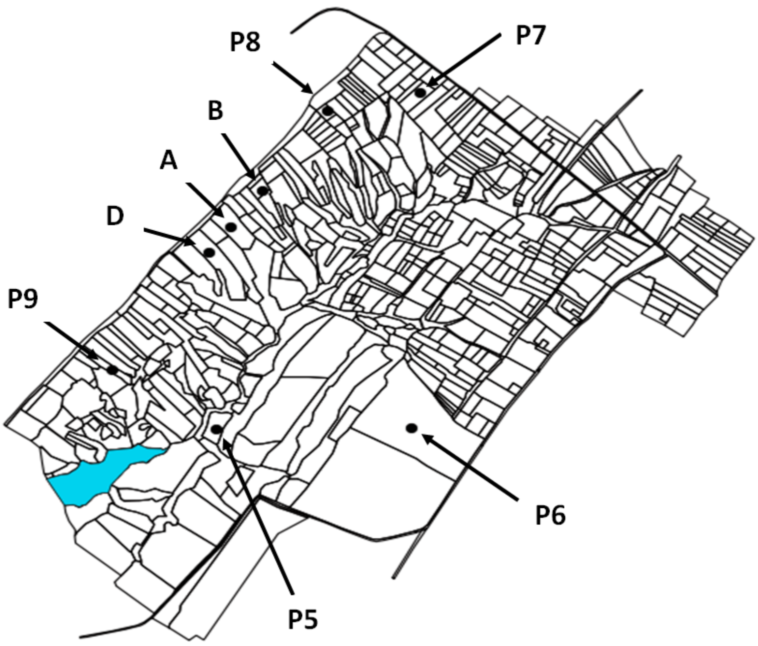

__Fig. 1.__ Map of the Kamech catchment with the location of the plots A, B, D, P5, P6, P7, P8 and P9. The meteorological station is located near the outlet of the catchment area, downstream limit of the hilly lake.

3.2.1. AquaCrop input data

3.2.1.1. Climatic data

The climatic data were collected by the meteorological station located near the outlet of the catchment area (see Fig. 1). First, ET_0 was calculated at the half-hourly time step by using the FAO-56 method along with measurements of solar radiation, air temperature, air humidity and wind speed. Next, estimates calculated at the half-hourly time step were integrated at the daily timescale.

All rainfall data were collected at a daily time step. The rain gauge for each of the plots P5, P6, P7, P8 and P9 was located downstream of the plot. For plots A, B and D, we used the data collected by the rain gauge located downstream of plot A, thanks to their spatial proximity. In the case of missing data, we used average values across all rain gauges within the catchment area.

3.2.1.2. Soil hydrodynamic parameters

AquaCrop inputs include soil depth and soil moisture at wilting point (HWP) and at field capacity (HFC). We consider three soil classes: Vertisols for plots A, B, D and P5, Cambisols for plots P6, P7, and P8 and Luvisols for plot P9. Soil depth and hydrodynamic parameters for each plot are shown in Table 2.

We summarize in this section the estimation of HWP and HFC; a detailed description is provided in Section 1 of the supplementary materials. We used the laboratory measurements (Cassel and Nielsen, 1986) conducted within the framework of the OMERE Observatory, and the agroclimatic method (Sreelash et al., 2017) with discrete soil moisture measurements conducted at specific dates. The comparison of the estimates resulting from these two approaches showed relative differences of approximately 15% on average (Table SP1 in supplementary materials), which corresponds to the precision and spatial representativeness of local field measurements, approximately 15% (Susha Lekshmi et al., 2014; Walker et al., 2004; Robinson et al., 2008). Next, we verified the consistency of the HWP and HFC estimates with the time series of SWC (SWC data are presented in Section 3.3.6). This led to the use of the estimates from the laboratory measurements for plot A, and to the estimates from the agroclimatic method for the other plots.

Table 2. *Soil characteristics of the plots. Soil classes are taken from Mekki et al. (2006). We used the same values of soil depth for plots A, B and D thanks to their spatial proximity.*

Plot	**Class**	**Soil depth**	**Soil hydrodynamic parameters (m^3/m^3)**	
			HWP	**HFC**
P5	Vertisol	1.60	0.23	0.45
P6	Cambisol	1.50	0.21	0.35
P7	Cambisol	1.60	0.23	0.44
P8	Cambisol	1.20	0.19	0.46
P9	Luvisol	1.60	0.25	0.47
A	Vertisol	1.15	0.34	0.43
B	Vertisol	1.15	0.26	0.44
D	Vertisol	1.15	0.23	0.44

3.2.1.3. Crop parameters

We chose wheat/barley, oats and faba bean as representative species of grain cereals, fodder cereals and legumes, respectively. In the literature, there are some annual crops for which AquaCrop parameterizations are not representative of various agro-environmental conditions. Indeed, some parameterizations are proposed in the literature for chickpeas (Mubvuma et al., 2021), leafy vegetables (Nyathi et al., 2018), table grape (Er-Raki et al., 2021), oats and faba bean (Yuan et al., 2013; Zeleke, 2019), but they need to be tested and confirmed in other geo-climatic contexts and for other crop varieties to ensure that they are reliable, as is the case for those related to wheat or corn crops.

For wheat, barley and faba bean, we used parameters proposed in the literature that were rather suitable for the local varieties of our study site, as indicated in Table 2 of Alaya et al. (2019). For oats, we used the values proposed by Yuan et al. (2013) for the conservative parameters (invariant from one variety to another), and we used values related to wheat for the nonconservative parameters that describe the phenological stages throughout the crop cycle, due to the lack of data.

3.2.2. AquaCrop multicriteria assessment

3.2.2.1. Actual evapotranspiration (ET_a)

For actual evapotranspiration, two datasets were available (Table 1): the first dataset was collected in plot A in 2013 for wheat, and the second dataset was collected in plot B in 2005 for oats. The time series were collected at the plot scale, with a 30 min timescale throughout the crop cycle. The daily ET_a measurements were derived from the energy balance closure method in 2005 (Zitouna-Chebbi et al., 2015) and from the eddy covariance method in 2013 (Boudhina et al., 2017a). For 2013, the missing latent heat flux data were reconstructed using the REddyProc gap-filling method (Reichstein et al., 2005). The experimentation, calibration, data processing and gap-filling are discussed in detail by Zitouna-Chebbi (2009); Zitouna-Chebbi et al., (2012; 2015; 2018), and Boudhina et al., (2017a, 2017b, 2018). ET_a data were finally aggregated at the daily timescale.

3.2.2.2. Crop variables (CC, AGB)

When dealing with vegetation growth throughout the crop cycle, we used planimetric measurements of the leaf area index (LAI) for cereals (wheat, barley, oats) and visual estimates of canopy cover (CC) for faba bean (Table 1). Nevertheless, AquaCrop simulates CC to describe crop growth. For cereals, we therefore converted LAI measurements into CC estimates by using Equation 1, as done in numerous studies (Katerji et al., 2013; Yuan et al., 2013; Pereira et al., 2015):

$$CC = 1 - e^{-k \times LAI} \qquad \text{(Equation 1)}$$

Coefficient k is an extinction coefficient that quantifies the light interception by canopy cover (Pereira et al., 2015). We used a k value equal to 0.57 for all cereals. The determination of this k value is discussed in Section 2 of the supplementary materials.

We also used measurements of dry aboveground biomass (AGB), except for barley in plot D in 2006. For each of the eight datasets, AGB was determined throughout the crop cycle using a destructive method (i.e., field samples to be weighed before and after oven drying). Spatial sampling varied across datasets, ranging from three to 10 replicates (Mekki, 2003; Boudhina et al., 2019). For each crop, the number of observation dates also varied across datasets, between three and 11 dates at maximum.

3.2.2.3. Soil water content (SWC)

Time series of SWC measurements were available for all datasets (Table 1). For 2001, 2002 and 2013, measurements were made using a neutron probe with a weekly frequency. For 2005 and 2006, measurements were made by the gravimetric method, with a biweekly frequency throughout the crop cycle and with a bimonthly frequency during summer with bare soil. All measurements were carried out across 1 m depth profiles. To account for spatial variability in SWC, the samples were collected at different landscape positions (distributed across the top, middle and bottom of each plot), except for 2001 and 2002, with one measurement only per plot. The moisture values were obtained by plot-scale averaging of measurements. Detailed descriptions of the measurements are given in Mekki (2003); Zitouna-Chebbi (2009); Boudhina et al. (2019).

3.2.2.4. Runoff (R)

Runoff measurements were included in each of the datasets listed in Table 1, apart from oats in 2005 and barley in 2006. Runoff data were collected at the daily timescale.

- For 2001 (end of December) and 2002 (November), runoff was measured in each plot using a 2 m² size harvesting frame that was connected to a tank with a 20-litre capacity (Mekki et al., 2006).
- For 2013, runoff was measured by the hydrological station located at the outlet of plot A. The experimental protocol is detailed in Inoubli et al. (2017).

3.3. Determination of initial soil moisture and fertilization degree

To obtain reliable AquaCrop simulations throughout the crop cycle for each of the nine datasets (Table 1), it was necessary to set the initial soil water content (SWC_i). It was also necessary to set the fertilization rate (FR) for cereal crops, while no fertilization rate was required for faba bean that is a nitrogen-fixing legume crop (FR represents the effect of the soil nutrient level on canopy development and biomass production, and AquaCrop expresses the lack of soil nutrient from soil fertility stress, by means of stress coefficients). Given that no information was available for either SWC_i or FR, we determined them by minimizing the differences between observations and simulations of CC, AGB and SWC (time series of ET_a were available for only two datasets).

For each of the nine datasets, we choose 15 SWC_i values between HWP and HFC and 30 FR values ranging from 70 to 100% according to expert knowledge. We then created pairs (SWC_i, FR) and generated the corresponding AquaCrop simulations. The optimal (SWC_i, FR) pair was selected using two criteria. First, the NRMSE (normalized root mean square error) had to be lower than 15% for SWC, which corresponds to measurement error on soil moisture (Susha Lekshmi et al., 2014). Second, we minimized the quadratic error between the observations and simulations of CC and AGB simultaneously using the objective function F defined by Equation 2 (Montes et al., 2014):

$$F = NRMSE_{CC}^{1/2} + NRMSE_{AGB}^{1/2} \qquad \text{(Equation 2)}$$

AquaCrop tends to overestimate CC observations during the senescence phase in the case of heat waves (Andarzian et al., 2011), while early senescence is recurrent in Kamech. To avoid the influence of any overestimation when minimizing the quadratic error, we calculated F over a simulation period that spread from the beginning of the crop growth to the maximum plant cover (CC = CC_max). Across the selected AquaCrop simulations, the obtained SWC_i values were larger than $0.75 \times$ HFC, and those retained for FR were approximately 85%. According to expert opinions, the FR values are representative of actual field conditions in the Kamech watershed.

3.4. Model evaluation

AquaCrop was evaluated by comparing simulations against observations throughout the crop cycle related to each of the nine datasets by considering the variables listed in Table 1 and related to vegetation (AGB, CC), water fluxes (ET_a, runoff as infiltration excess), and water storage (SWC). Table 1 details the available data used for each crop, year and plot.

For the statistical evaluation of the simulations against observations, we selected the following indicators: coefficient of determination (R^2), root mean square error (RMSE), normalized root mean square error (NRMSE) and mean bias error (MBE). These are commonly used in the literature for evaluating numerical models (Kustas et al., 1996; Jacob et al., 2002), including hydrological (Moriasi et al., 2015) or crop (Yang et al., 2014) models. We also used the Student's t test for linear regressions on model validation, to test the null hypothesis (slope and offset can be equal to 1 and 0, respectively). If the critical values (p value) were larger than 5%, then the null hypothesis could not be rejected with 95% confidence, and model performances could be considered satisfactory.

$$R^2 = \frac{\sum_{i=1}^{n}\left(P_i - \overline{O}\right)^2}{\sum_{i=1}^{n}\left(O_i - \overline{O}\right)^2} \qquad \text{(Equation 3)}$$

$$RMSE = \sqrt{\frac{\sum_{i=1}^{n}(Pi - Oi)^2}{n}} \qquad \text{(Equation 4)}$$

$$NRMSE = \frac{RMSE}{\overline{O}}\ x\ 100 \qquad \text{(Equation 5)}$$

$$MBE = \frac{\sum_{i=1}^{n}(Pi - Oi)}{n} \qquad \text{(Equation 6)}$$

where Pi and Oi, are the simulated and observed variables at time step i, respectively. Ō is the averaged value of the observations, and n is the observation number.

MBE indicates whether the model simulations underestimate or overestimate the observations. NRMSE gives an indication of the relative difference between simulations and observations. According to Jamieson et al. (1991), a crop model is classified as excellent if NRMSE < 10%, good if NRMSE ∈ [10% - 20%[, acceptable if NRMSE ∈ [20% - 30%[and poor if NRMSE > 30%. Likewise, simulations are considered acceptable if the coefficient of determination R^2 is greater than 0.5. For runoff, we did not consider the NRMSE in the evaluation of the AquaCrop simulations because of the low values of this variable, which give very high NRMSE values (> 100%) that are difficult to interpret.

4. Results

4.1. Canopy cover (CC)

According to the comparison between AquaCrop simulations and in situ measurements of CC (Fig. 2 and Table 3), for each crop type, AquaCrop simulations overestimated observations for cereals and underestimated them for faba bean, with a positive MBE ranging between 0.03 and 0.23 for cereals and a negative MBE (-0.02) for faba bean. The R^2 values did not exceed 0.4, apart from faba bean (0.9). The RMSE values varied between 0.11 (29% relative) and 0.37 (75% relative), with the lowest values being observed for faba bean. For wheat and faba bean, the t test provided p values larger than 5% on slope and offset. For barley, the t test provided p value lower than 5% on slope and offset. For oats, the t test provided a p value lower than 5% on offset only.

To study these results in detail, we analysed the temporal evolution of CC for each simulation throughout the corresponding crop cycle (Fig. SP2 in Section 3 of the supplementary materials). For wheat in 2002, oats in 2005, and barley in 2006, the temporal evolution of the canopy cover simulated by the model showed acceptable estimates during the crop growth phase, despite an overestimation of CC observations during the senescence phase. For wheat in 2013, AquaCrop underestimated observations between DAS (day after sowing) 25 and DAS 120, and it overestimated them at the end of the crop cycle. For oats in 2002, the model underestimated observations throughout the crop cycle. Most time series suggested that AquaCrop simulated senescence with delay compared to observations.

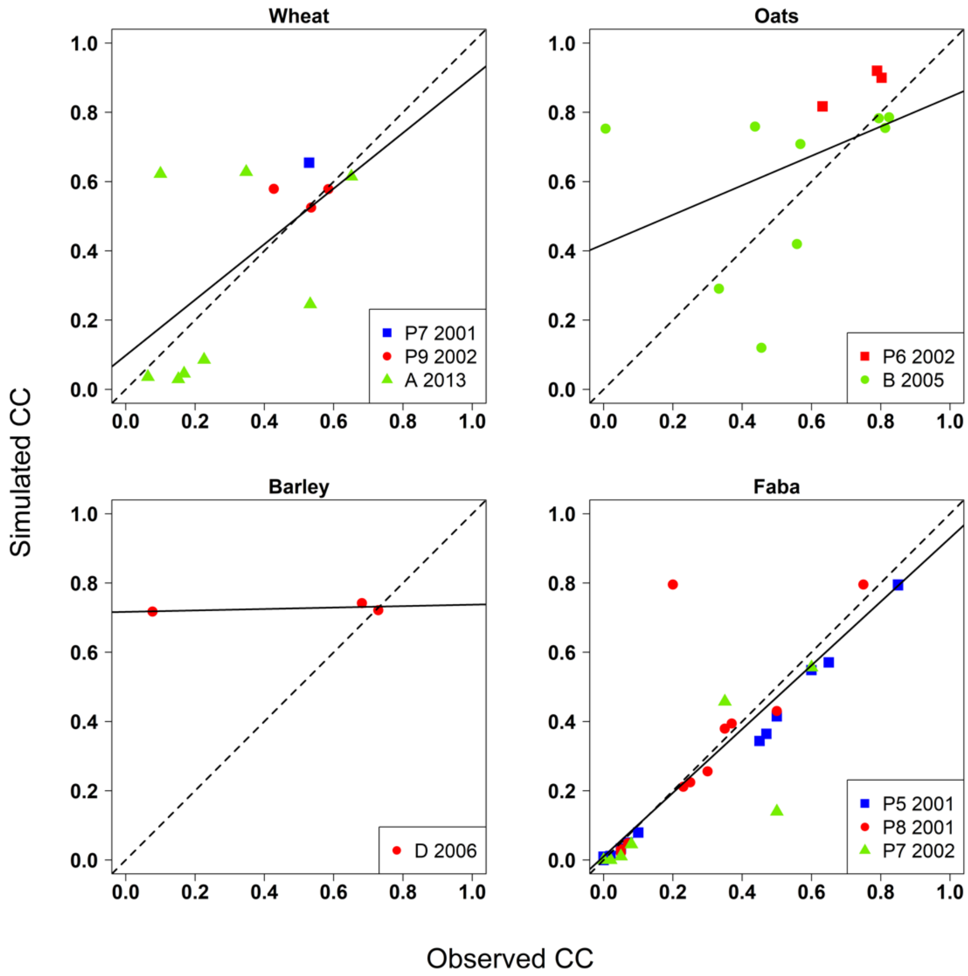

Fig. 2. *Comparison between simulated and observed canopy cover (CC) on a crop type basis. Each scatterplot corresponds to a crop type for several years and/or several plots. Each dataset is indicated by a different marker and a different colour. Px, A, B, D relates to plots and YYYY to years. The black line corresponds to the regression line, and the black dashed line corresponds to the 1:1 line.*

Table 3. *Statistical indicators when comparing simulations against observations for canopy cover (CC) on a crop type basis. n is the observation number.* R^2 *is the correlation coefficient. The t test corresponds to the p value of the Student's t test. The statistical indicators RMSE, NRMSE and MBE are defined in Section 3.4.*

Crop	Var	n	R^2 (-)	Offset (-)		Slope (-)		RMSE (-)	NRMSE (%)	MBE (-)
				Value	t test	Value	t test			

Wheat	CC	12	0.39	0.10	0.47	0.80	0.55	0.21	58	0.03
Oats		12	0.18	0.42	0.04	0.43	0.08	0.27	46	0.08
Barley		3	0.33	0.72	0.02	0.02	0.02	0.37	75	0.23
Faba		38	0.86	0.01	0.73	0.92	0.21	0.12	32	-0.02

For each soil class, the comparison between AquaCrop simulations and in situ measurements of CC (Fig. 3 and Table 4) showed that AquaCrop simulations overestimated observations for the three soil classes. Additionally, the agreement between the model simulations and in situ measurements was moderate, with either (1) large R^2 values (0.59 and 0.8) but large RMSE values (0.15 and 0.21, corresponding to 41% and 48% relative, respectively) or (2) a moderate RMSE value (0.09, 18% relative) but a low R^2 value (0.05). Nevertheless, it was difficult to conclude for Luvisols because of the dataset size, with only one plot and one year. Conversely, the results for both Vertisols and Cambisols were similar, with relative changes in statistical indicators of approximately 25%. Apart from t test on slope for Vertisols, all p values were larger than 5%.

Finally, we could not conclude on any possible trend to over- or under- estimation according to the magnitude of observations. Indeed, the regression slope could be larger or lower than one from one soil class to another, in contrast to results reported on a crop type basis for which the regression slope was systematically lower than one.

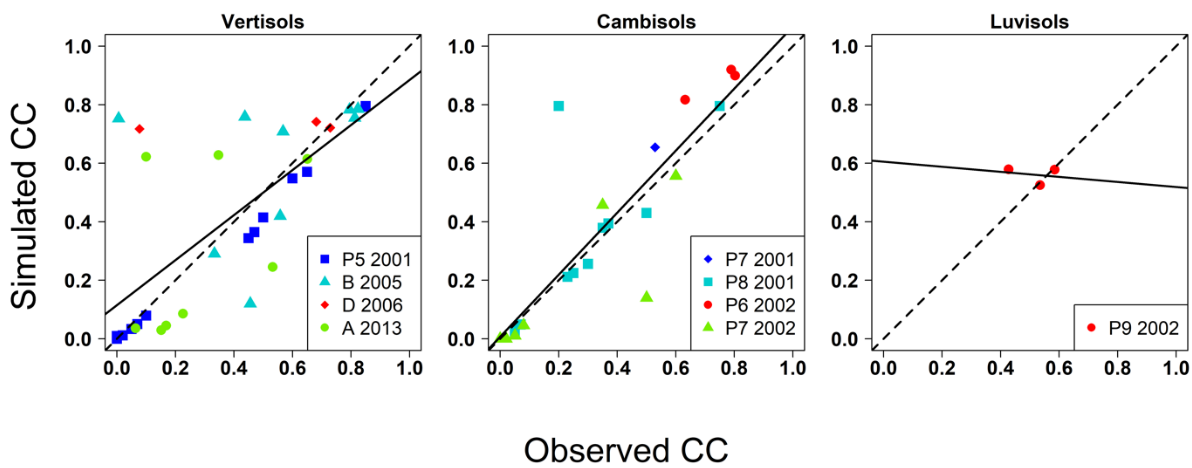

Fig. 3 Comparison between simulated and observed canopy cover (CC) on a soil class basis. Each scatterplot corresponds to a soil class for several plots, years and crops. Each dataset is indicated by a different marker and a different colour. Px, A, B, D relates to plots and YYYY to years. The black line corresponds to the regression line, and the black dashed line corresponds to the 1:1 line.

Table 4. *Statistical indicators when comparing simulations against observations for canopy cover (CC) on a soil class basis. n is the observation number. R^2 is the correlation coefficient. The t test corresponds to the p value of the Student's t test. The statistical indicators RMSE, NRMSE and MBE are defined in Section 3.4.*

Soil	**Var**	**n**	**R^2 (-)**	**Offset (-)**		**Slope (-)**		**RMSE (-)**	**NRMSE (%)**	**MBE (-)**
				Value	**t test**	**Value**	**t test**			
Vertisols	CC	39	0.59	0.12	0.05	0.77	0.03	0.21	47	0.01
Cambisols		23	0.76	0.01	0.90	1.06	0.64	0.16	45	0.03
Luvisols		3	0.05	0.61	0.20	-0.09	0.21	0.09	17	0.05

4.2. Aboveground biomass (AGB)

The comparison between simulated and observed AGB (Fig. 4 and Table 5), for each crop type, showed a good estimation of this variable by the model for cereals, with R^2 approximately 0.95 and RMSE approximately 0.6 ton ha^{-1} (16% relative). For faba bean, the simulations were less good, with $R^2 = 0.52$ and RMSE = 1.4 ton ha^{-1} (46% relative). The bias values indicated that AquaCrop tended to overestimate AGB observations for cereals (MBE > 0) and to underestimate them for faba bean (MBE < 0). For all crop types, the t test provided p values larger than 5%.

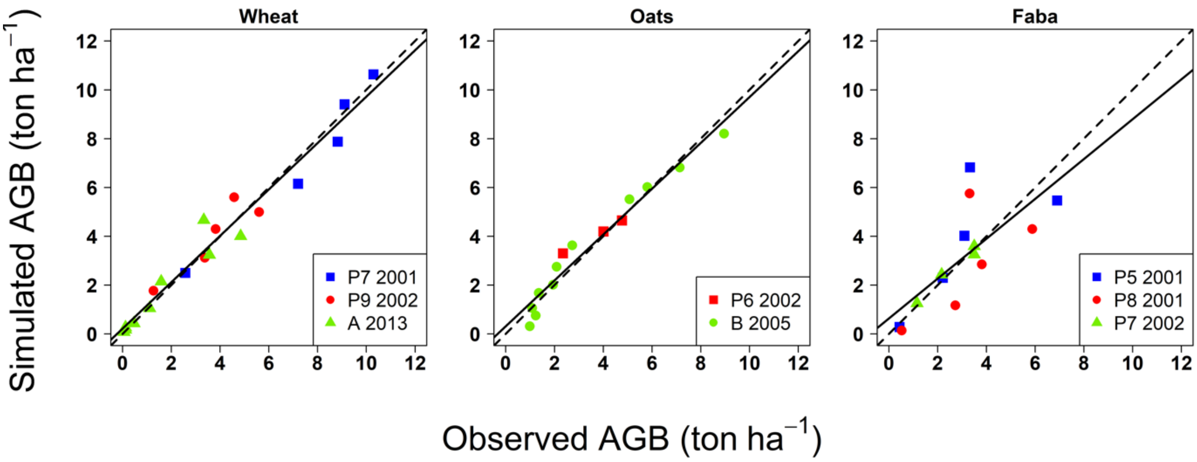

Fig. 4. *Comparison between simulated and observed aboveground biomass (AGB) on a crop type basis. Each scatterplot corresponds to a crop type for several years and/or several plots. Each dataset is indicated by a different marker and a different colour. Px, A, B, D relates to plots and YYYY to years. The black line corresponds to the regression line, and the black dashed line corresponds to the 1:1 line.*

Table 5. *Statistical indicators when comparing simulations against observations for above-ground biomass (AGB) on a crop type basis. n is the observation number. R^2 is the correlation coefficient. The t test corresponds to the p value of the Student's t test. The statistical indicators RMSE, NRMSE and MBE are defined in Section 3.4.*

Crop	Var	n	R^2 (-)	Offset (ton ha^{-1})		Slope (-)		RMSE (ton ha^{-1})	NRMSE (%)	MBE (ton ha^{-1})
				Value	t test	Value	t test			
Wheat	AGB	19	0.96	0.22	0.34	0.95	0.30	0.61	16	0.03
Oats		14	0.95	0.31	0.25	0.94	0.33	0.53	15	0.10
Faba		14	0.52	0.64	0.44	0.82	0.43	1.40	46	0.08

To better understand the poor results for faba bean, Fig. SP3 displays the temporal evolution of AGB for both cereal crops and faba bean during the crop cycle. We noted that AquaCrop appropriately simulated AGB for 2002 in plot P7. For the year 2001 in plots P5 and P8, the model acceptably simulated AGB at the beginning of the crop cycle until Day 125 after sowing, but it overestimated observations at the end of the crop cycle. This could explain the low R^2 value given in Table 5.

The comparison between AquaCrop simulations and in situ measurements of AGB (Fig. 5 and Table 6) for each soil class, showed that AquaCrop simulated AGB well for the 3 soil classes. Bias values indicated that the model tended to overestimate observations for Vertisols and Luvisols (MBE > 0) and to underestimate them for Cambisols (MBE < 0). The R^2 values were above 0.84, with a small relative variation of 6% across the 3 soil classes. The RMSE values were between 0.62 ton ha^{-1} (17% relative) and 0.95 ton ha^{-1} (21% relative). Additionally, all regression slopes were close to one, as was the case when analysing results on a crop type basis. This outcome agreed with the results of the t test that provided p values larger than 5% for all soil classes.

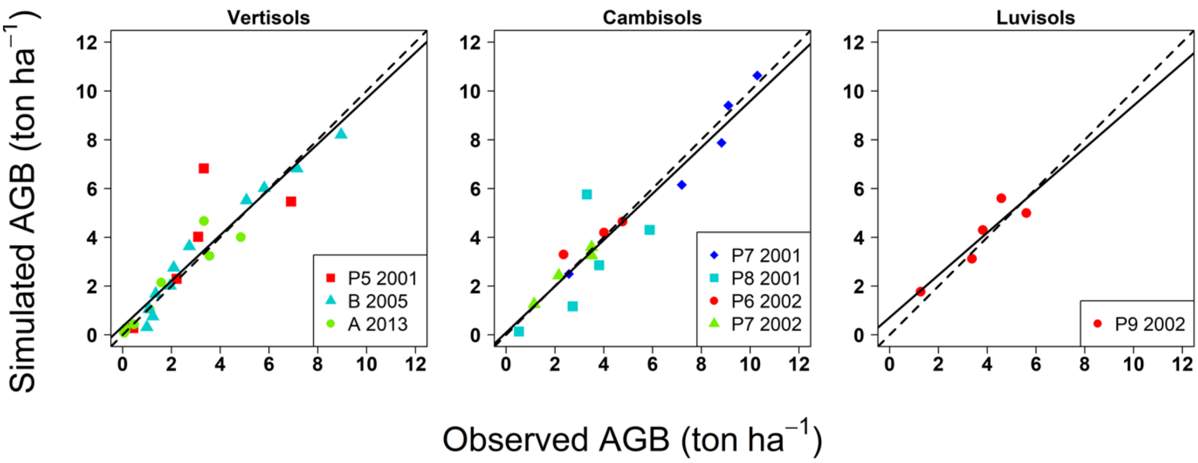

Fig. 5. *Comparison between simulated and observed aboveground biomass (AGB) on a soil class basis. Each scatterplot corresponds to a soil class for several plots, years and crops. Each dataset is indicated by a different marker and a different colour. Px, A, B, D relates to plots and YYYY to years. The black line corresponds to the regression line, and the black dashed line corresponds to the 1:1 line.*

Table 6. *Statistical indicators when comparing simulations against observations for above-ground biomass (AGB) on a soil class basis. n is the observation number. R^2 is the correlation coefficient. The t test corresponds to the p value of the Student's t test. The statistical indicators RMSE, NRMSE and MBE are defined in Section 3.4.*

Soil	**Var**	**n**	**R^2 (-)**	**Offset (ton ha^{-1})**		**Slope (-)**		**RMSE (ton ha^{-1})**	**NRMSE (%)**	**MBE (ton ha^{-1})**
				Value	**t test**	**Value**	**t test**			
Vertisols	AGB	25	0.86	0.35	0.24	0.94	0.42	0.92	33	0.17
Cambisols		17	0.89	0.10	0.83	0.95	0.56	0.95	21	-0.13
Luvisols		5	0.84	0.72	0.47	0.87	0.59	0.62	17	0.23

4.3. Actual evapotranspiration (ET_a)

As shown in Table 1, ET_a measurements were only available for oats in 2005 (plot B) and for wheat in 2013 (plot A). The comparison between AquaCrop simulations and in situ measurements of ET_a (Fig. 6 and Table 7) showed a slight overestimation of the observations. The overestimation was more important for oats (MBE = 0.28 mm day^{-1}) than for wheat (MBE = 0.17 mm day^{-1}). The other indicators showed that the model performance was acceptable for both crops, with $R^2 \geq 0.6$ and RMSE $\leq$ 0.84 mm day^{-1} (35% relative on average). Additionally, we noted scatterings around the regression lines that were close to the 1:1 line. Apart from slope for wheat, the t test provided p values lower than 5%.

Table 7. *Statistical indicators when comparing simulations against observations for actual evapotranspiration (ET_a) on a crop type basis. n is the observation number. R^2 is the correlation coefficient. The t test corresponds to the p value of the Student's t test. The statistical indicators RMSE, NRMSE and MBE are defined in Section 3.4.*

Crop	**Var**	**n**	**R^2 (-)**	**Offset (mm day^{-1})**		**Slope (-)**		**RMSE (mm day^{-1})**	**NRMSE (%)**	**MBE (mm day^{-1})**
				Value	**t test**	**Value**	**t test**			
Wheat	ET_a	134	0.59	0.54	0	0.82	0	0.69	33	0.17
Oats		150	0.64	0.33	0.03	0.98	0.72	0.84	38	0.28

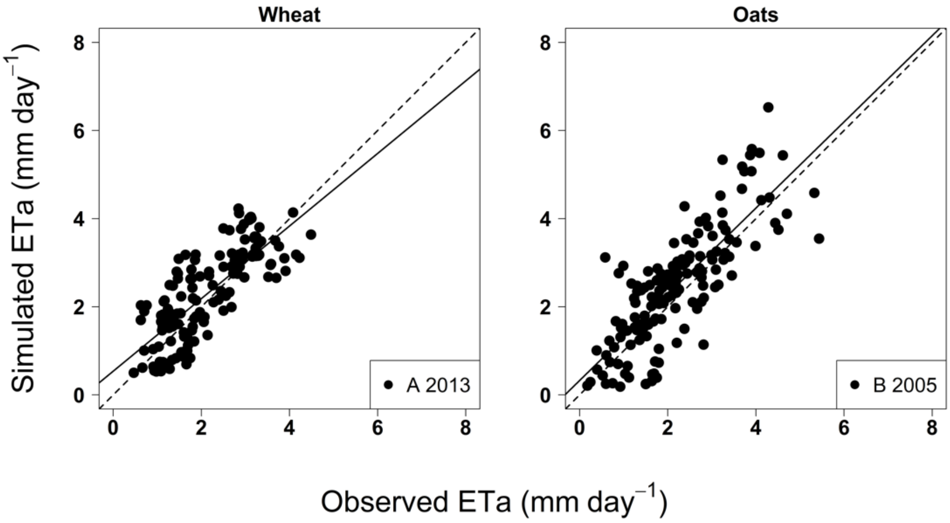

Fig. 6. *Comparison between simulated and observed actual evapotranspiration (*ET_a*) on a crop type basis. Each scatterplot corresponds to a crop type. A, B relates to plots and YYYY to years. The black line corresponds to the regression line, and the black dashed line corresponds to the 1:1 line.*

For a better understanding of the scattering around the regression line, we investigated the temporal dynamics of ET_a simulations by AquaCrop throughout the crop cycle for wheat and oats (Fig. SP4). We observed a significant similarity between the simulated and observed temporal evolutions of ET_a for both crops. For wheat, the overestimation of ET_a observations by model simulations was more important from DAS 130 (9 Mar 2013). For oats, we observed an overestimation of ET_a observations by the model between DAS 140 – (3 May 2005) and DAS 160 - (23 May 2005) – as well as an underestimation of the observations from DAS 160 until the end of the crop cycle. Overall, we did not observe any trend to under- or overestimation according to crop phenological stages.

The two datasets of ET_a belonged to the Vertisols class. The statistical indicators we obtained when merging the scatterplots in Fig. 6 suggested good model performance in simulating ET_a, with acceptable values for the correlation coefficient (0.62) and RMSE (0.77 mm day^{-1}) and a slight overestimation of ET_a observations by model simulations (MBE = 0.23 mm day^{-1}).

4.4. Runoff (R)

For runoff (infiltration excess), in situ measurements were available for all datasets, except for barley in plot D in 2006 and oats in plot B in 2005 (Table 1). The comparison between AquaCrop simulations and in situ measurements (Fig. 7 and Table 8) for each crop type showed that the model overestimated observations. The magnitude of the overestimation varied from one crop to another, and it was larger for oats (MBE = 0.2 mm day^{-1}). AquaCrop acceptably simulated runoff for wheat and faba bean, with R^2 values larger than 0.8 and RMSE values lower than 0.63 mm day^{-1}. The simulations were less effective for oats (R^2 = 0.41; RMSE = 1.44 mm day^{-1}). According to Fig. 7, the overestimation of runoff observations by AquaCrop simulations mainly occurred for low runoff values. For wheat in 2013 in plot A, the model acceptably simulated a significant runoff event (27 mm day^{-1}) with a slight underestimation. For all crops, the t test on slope provided p values equal to 0. Apart from wheat, the t test on offset provided p values larger than 5%.

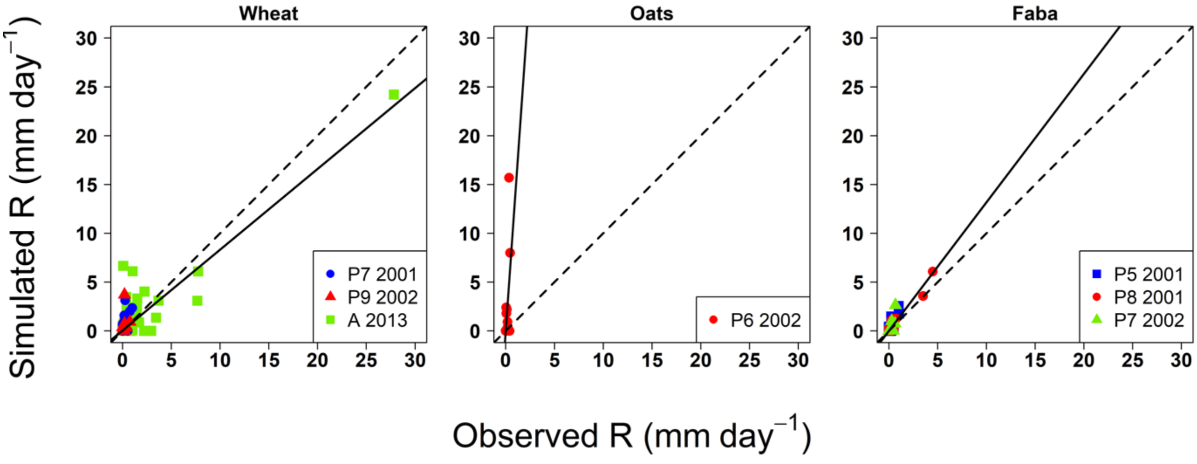

Fig. 7. *Comparison between simulated and observed runoff (R) on a crop type basis. Each scatterplot corresponds to a crop type for several years and/or several plots. Each dataset is indicated by a different marker and a different colour. Px, A, B, D relates to plots and YYYY to years. The black line corresponds to the regression line, and the black dashed line corresponds to the 1:1 line.*

Table 8. *Statistical indicators when comparing simulations against observations for runoff (R) on a crop type basis. n is the observation number.* R^2 *is the correlation coefficient. The t test corresponds to the p value of the Student's t test. The statistical indicators RMSE, NRMSE and MBE are defined in Section 3.4.*

Crop	**Var**	**n**	**R^2 (-)**	**Offset (mm day^{-1})**		**Slope (-)**		**RMSE (mm day^{-1})**	**MBE (mm day^{-1})**
				Value	**t test**	**Value**	**t test**		
Wheat	R	478	0.80	0.06	0.03	0.83	0	0.63	0.02
Oats		147	0.41	-0.03	0.76	14.26	0	1.44	0.20
Faba		453	0.84	0.01	0.25	1.32	0	0.19	0.02

For a better understanding of these scatterplots, Fig. SP5 displays the temporal evolution of observed and simulated runoff for each dataset. Apart from wheat in plot A in 2013, the observed runoff was usually low, with values below 15 mm day^{-1}. The most important differences between observed and simulated accumulations were noted for wheat in plot P7 in 2001 (12 mm day^{-1}) and for oats in plot P6 in 2002 (29 mm day^{-1}). We also noted that the model simulated large runoff values at the beginning of the crop cycle compared to in situ measurements. This was true for wheat in plot P9 in 2002 and in plot A in 2013, as well as for oats in plot P6 and faba bean in plot P7 in 2002. The same trend was also observed at the end of the crop cycle (the last 40 days) for oats in plot P6 in 2002 and wheat in plot A in 2013.

From the comparison between AquaCrop simulations and in situ measurements of runoff, for each soil class (Fig. 8 and Table 9) we noted a better performance of the model for Vertisols (R^2 = 0.82, RMSE = 0.71 mm day^{-1}), where the large R^2 value for Vertisols likely results from a single large runoff event. The model performed worse for Cambisols (R^2 = 0.22 and RMSE = 0.76 mm day^{-1}) and Luvisols (R^2 = 0.21 and RMSE = 0.28 mm day^{-1}). The t test provided p values larger than 5% and lower than 5% for offset and slope, respectively.

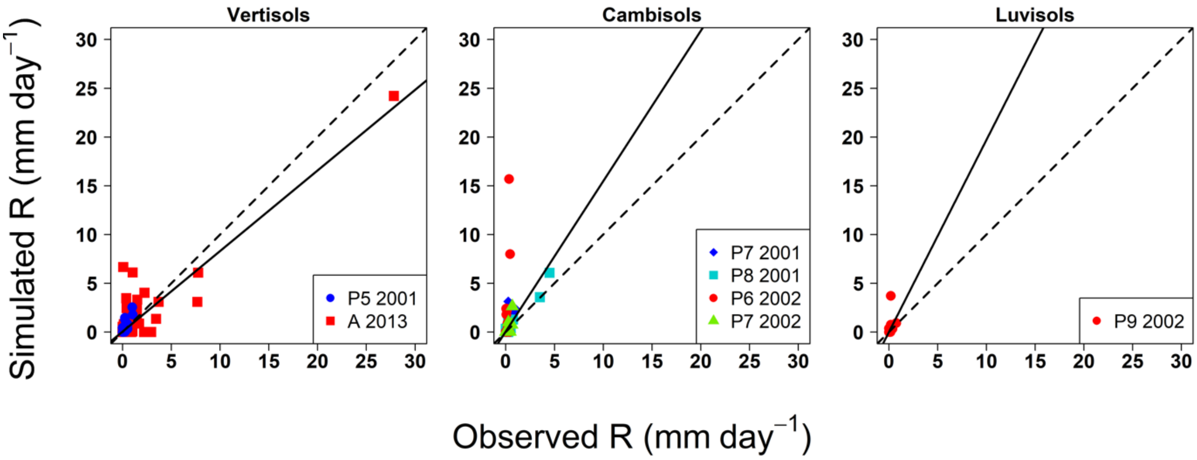

Fig. 8. *Comparison between simulated and observed runoff (R) on a soil class basis. Each scatterplot corresponds to a soil class for several plots, years and crops. Each dataset is indicated by a different marker and a different colour. Px, A, B, D relates to plots and YYYY to years. The black line corresponds to the regression line and the black dashed line corresponds to the 1:1 line.*

Table 9. *Statistical indicators when comparing simulations against observations for runoff (R) on a soil class basis. n is the observation number. R^2 is the correlation coefficient. The t test corresponds to the p values of the Student's t test. The statistical indicators RMSE, NRMSE and MBE are defined in Section 3.4.*

Soil	**Var**	**n**	**R^2 (-)**	**Offset ($mm\ day^{-1}$)**		**Slope (-)**		**RMSE ($mm\ day^{-1}$)**	**MBE ($mm\ day^{-1}$)**
				Value	**t test**	**Value**	**t test**		
Vertisols	R	331	0.82	0.05	0.15	0.83	0	0.71	0.01
Cambisols		587	0.22	0.06	0.07	1.54	0	0.76	0.08
Luvisols		160	0.21	0.01	0.61	1.97	0	0.28	0.03

4.5. Soil water content (SWC)

From the comparison between AquaCrop simulations and in situ measurements of soil water content (SWC) (Fig. 9 and Table 10), for each crop type, we noted that AquaCrop simulated this variable very well, with R^2 values between 0.76 and 0.95 and RMSE values between 18.5 mm and 32 mm. The best simulations were observed with oats. The MBE values indicated that the model simulations slightly underestimated the SWC observations for oats and faba beans and slightly overestimated them for wheat and barley. Despite these favourable results, we noted that the regression slope could be far from the 1:1 line for wheat. Additionally, we could not conclude on any possible trend to over- or underestimation according to the magnitude of in situ measurements. Indeed, the regression slopes were lower than one, apart from oats (1.04). For oats and barley, the t test provided p values larger than 5%. For wheat, the t test provided p value lower than 5%. For faba bean, the t test provided a p value lower than 5% for slope.

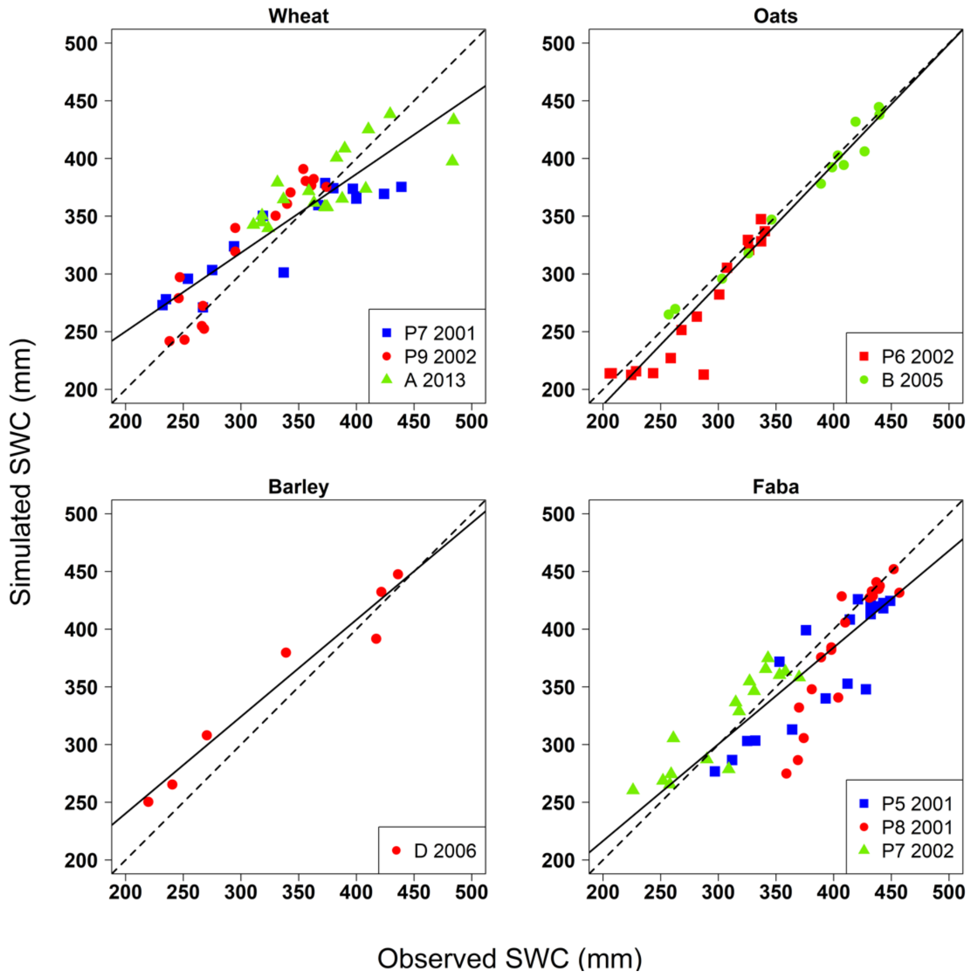

Fig. 9. *Comparison between simulated and observed soil water content (SWC) on a crop type basis. Each scatterplot corresponds to a crop type for several years and/or several plots. Each dataset is indicated by a different marker and a different colour. Px, A, B, D relates to plots and YYYY to years. The black line corresponds to the regression line, and the black dashed line corresponds to the 1:1 line.*

Table 10. *Statistical indicators when comparing simulations against observations for soil water content (SWC) on a crop type basis. n is the observation number.* R^2 *is the correlation coefficient. The t test corresponds to the p values of the Student's t test. The statistical indicators RMSE, NRMSE and MBE are defined in Section 3.4.*

Crop	Var	n	R^2 (-)	Offset (mm)		Slope (-)		RMSE (mm)	NRMSE (%)	MBE (mm)
				Value	t test	Value	t test			

Wheat	SWC	52	0.77	113.86	0	0.68	0	30.93	9	5.33
Oats		30	0.95	-21.70	0.14	1.04	0.33	18.51	6	-8.05
Barley		7	0.95	72.63	0.05	0.84	0.11	28.17	8	18.71
Faba		55	0.76	48.99	0.05	0.84	0.01	31.98	9	-11.71

The comparison between simulated and in situ measurements of SWC (Fig. 10 and Table 11), for each soil class, showed that the model well simulated SWC for the 3 soil classes, with a trend to underestimate observations for Vertisols and Cambisols and overestimate observations for Luvisols. The R^2 values were above 0.79, with a relative variation of approximately 12% across the three soil classes. The RMSE values ranged from 25 mm to 30 mm, and the regression slopes were lower than one, apart from Luvisols. For Luvisols, the t test provided p value larger than 5%. For Vertisols and Cambisols, the t test provided p values lower than 5%.

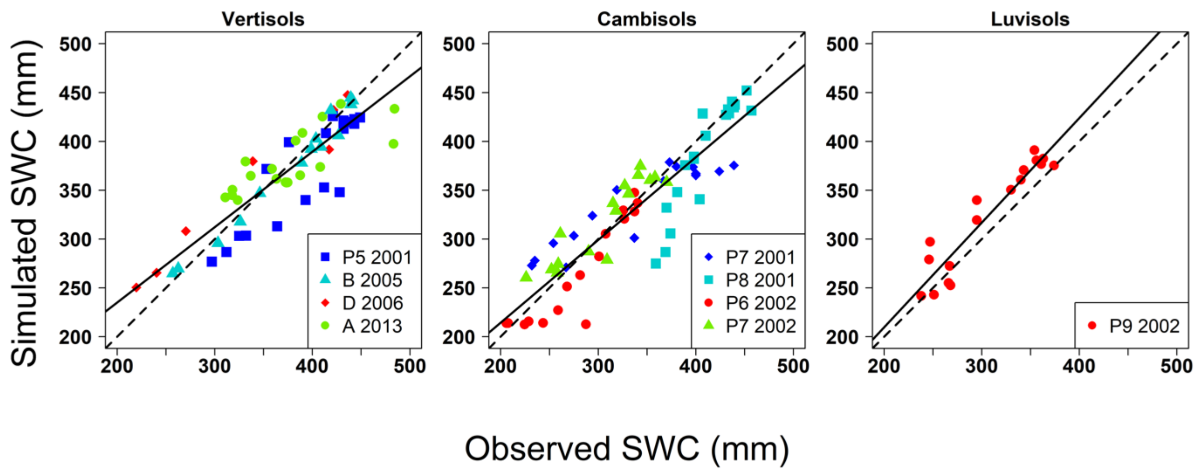

Fig. 10. *Comparison between simulated and observed soil water content (SWC) on a soil class basis. Each scatterplot corresponds to a soil class for several plots, years and crops. Each dataset is indicated by a different marker and a different colour. Px, A, B, D relates to plots and YYYY to years. The black line corresponds to the regression line, and the black dashed line corresponds to the 1:1 line.*

Table 11. *Statistical indicators when comparing simulations against observations for soil water content (SWC) on a soil class basis. n is the observation number. R^2 is the correlation coefficient. The t test corresponds to the p values of the Student's t test. The statistical indicators RMSE, NRMSE and MBE are defined in Section 3.4.*

Soil	**Var**	**n**	**R^2 (-)**	**Offset (mm)**		**Slope (-)**		**RMSE (mm)**	**NRMSE (%)**	**MBE (mm)**
				Value	**t test**	**Value**	**t test**			
Vertisols	SWC	59	0.79	80.77	0	0.77	0	28.41	8	-5.37
Cambisols		68	0.82	44.75	0.01	0.85	0	30.51	9	-6.69
Luvisols		17	0.89	-4.38	0.89	1.07	0.48	25.30	8	17.29

5. Discussion

5.1. Canopy cover (CC)

The large RMSE and NRMSE values on CC were ascribed to an overestimation of CC observations by AquaCrop simulations throughout the senescence phase. This overestimation could result from the fact that the model disregarded the effect of high temperatures on crop functioning during the senescence phase (Andarzian et al., 2011). First, AquaCrop accounted for the effect of heat stress (low and high temperatures) on the pollination and harvest index only. Second, the early senescence we observed was not due to water stress: the seasonal courses of ET_a and ET_0 observed for wheat in 2013 in plot A (Fig. SP4) started to diverge as of DAS 140 (19 Apr 2013), while senescence began at DAS 120 (30 Mar 2013). According to local farmers, early or sudden senescence of vegetation after heat waves has been observed in Kamech.

Other studies reported overestimations of field observations by AquaCrop for CC at the end of the crop cycle for wheat in arid / semiarid climates, with lower magnitudes (Andarzian et al., 2011; Sghaier et al., 2014; Toumi et al., 2016). Beyond such differences during the senescence, the method used to convert LAI to CC for cereals might be an additional source of uncertainty, since the conversion was calibrated on hemispherical photos and applied on planimetric measurements, both observation types leading to physical differences (Jonckheere et al (2005).

5.2. Aboveground Biomass (AGB)

AquaCrop simulated AGB well, with an overestimation trend at the end of the crop cycle (e.g., faba bean, Fig. SP3). This could be ascribed to the overestimation of CC observations by AquaCrop simulations during the senescence phase in relation to a possible delay in senescence by model simulations. For faba bean plot P5 in 2001, this could not be shown due to the lack of CC measurements at the end of the crop cycle. However, Fig. SP2 indicates a recurrent overestimation of CC observations by AquaCrop simulations at the end of the crop cycle for different crop types and soil classes. Other studies have reported an overestimation of AGB observations by AquaCrop simulations, either at the end of the crop cycle (Katerji et al., 2013; Ahmadi et al., 2015; Sandhu and Irmak, 2019) or during the growth phase (Sghaier et al., 2014).

5.3. Actual evapotranspiration (ET_a)

AquaCrop showed acceptable performance in simulating ET_a for wheat and oats, with a trend to slightly overestimate observations. The overestimation of ET_a from DAS 130 (9 April 2013) for wheat and DAS 140 (3 May 2005) for oats could be related to the overestimation of CC observations during the senescence. Masasi et al. (2019) reported a similar trend for sorghum in a semiarid climate, and they suspected large atmospheric evaporative demand and poor characterizations of soil hydrodynamic parameters. Despite this overestimation in ET_a, AquaCrop well reproduced the divergence between ET_a and ET_0 courses at the end of the crop cycle.

The differences between simulated and observed ET_a values could also be due to (1) the eddy covariance measurements that tend to underestimate ET_a (Boudhina et al., 2019; Leuning et al., 2012), and (2) the reconstruction of missing ET_a data that induces uncertainties (Boudhina et al., 2018; Zitouna-Chebbi et al., 2018). Besides, Katerji et al. (2013) recalled that the ET_a calculation method in AquaCrop has been subject to several criticisms, especially when applied in semiarid Mediterranean regions (Katerji and Rana, 2006; Lovelli et al., 2007). A first source of error is assuming a constant surface resistance, since several studies in semiarid and arid regions have shown that it leads to underestimating ET_0 compared to lysimeter measurements (Katerji and Rana 2006). A second source of error is using the default value proposed by Allen et al. (1998) for cultural coefficient Kc, since several works reported differences up to 40% between this value and those observed in situ (Katerji and Rana 2006).

In contrast to the present study, previous works reported an underestimation for ET_a by AquaCrop for maize and tomato (Katerji et al., 2013) and for wheat (Toumi et al., 2016) in a Mediterranean climate. No explanation could be found for this contradiction. For two calibration plots, Toumi et al. (2016) reported RMSE values of 0.47 mm day^{-1} and 0.69 mm day^{-1}, which were similar to the RMSE value found in the current study for wheat in 2013 in plot A.

5.4. Runoff (R)

For wheat in plot P7 in 2001, wheat in plot P9 in 2002, and oat in plot P6 in 2002, AquaCrop simulated significant runoff values on DAS 19 (3 Dec 2000), DAS 2 (13 Dec 2001), and DAS 12 (11 Dec 2001), respectively. However, we could not evaluate AquaCrop simulations before the second half of December, due to the lack of in situ measurements. However, it was possible to verify the potential occurrence of runoff. According to Mekki (2003), rainfall greater than 20 mm day^{-1} is likely to generate runoff, regardless of surface conditions. Thus, the rainfall recorded on DAS 19 for plot P7 in 2001, DAS 2 for plot P9 in 2002, and DAS 12 for plot P6 in 2002 were equal to 40 mm, 20 mm, and 28 mm, respectively (data not shown), which could have produced runoff. This was also consistent with the slight increase of outlet lake level in early December (compared to mid-November, data not shown). Overall, the runoff simulations by AquaCrop early in the crop cycle were consistent with observations and expert knowledge.

For wheat in plot P9 in 2002 (DAS 10, 21 Dec 2001), wheat in plot A in 2013 (DAS 9, 09 Dec 2012), and oats in plot P6 in 2002 (DAS 20, 19 Dec 2001), we noted large values of model-simulated runoff early in the crop cycle, but we did not observe coincident runoff events from field observations. We observed the same difference between simulated and unobserved peak runoff at the end of the crop cycle, for wheat in 2013 in plot A and for oats in 2002 in plot P6. This could be explained by the presence of shrinkage cracks, which are known to generate preferential infiltration at the expense of runoff (Inoubli et al., 2017).

Wolka et al (2021) reported one of the few assessments on the ability of AquaCrop to simulate runoff. They noted that AquaCrop simulated runoff with RMSE values ranging from 9.8 mm to 61.5 mm. However, it was difficult to compare these results with ours, because of larger rainfall and runoff accumulations for Wolka et al. (2021).

5.5. Soil water content (SWC)

AquaCrop showed good performance in simulating soil water content. For oats, the underestimation of SWC observations was ascribed to the overestimations of ET_a and runoff. The differences between simulations and observations could be due to (1) inaccurate soil moisture initialisations, (2) poor characterizations of soil hydrodynamic properties (HWP and HFC) and (3) inadequate AquaCrop formalisms when simulating water fluxes (ET_a, runoff, drainage). Additionally, disregarding capillary rise was not critical because most plots were located at slope tops and therefore relatively far from possible shallow aquifers. Overall, the errors in SWC simulations were ascribed to the characterization of soil hydrodynamic properties (HWP and HFC), given the accuracies of AquaCrop simulations for water fluxes and crop variables.

Previous studies reported overestimations of SWC observations by AquaCrop simulations, notably for wheat (Andarzian et al., 2011), maize (Nyakudya and Stroosnijder, 2014) and barley (El Mokh et al., 2017). These overestimations were often noticed during dry periods, which can be explained by constraints on SWC, since the latter cannot drop below HWP.

5.6. Analysis by crop type and soil class

When dealing with AquaCrop performance according to crop type, AquaCrop could be used for predicting crop growth and biomass production. Oat crops could be used as animal fodder, which is a common practice within Kamech and the surrounding region, with subsequent grazing and cutting operations throughout the crop cycle. However, AquaCrop does not account for the dynamics of the crop canopy induced by such agricultural practices. Nyathi et al (2018) tried to parameterize this practice for leafy vegetables, by performing independent simulations for any crop and assuming that the initial canopy cover (CC0) was reset according to the remaining canopy cover (from 1 to 2%) after each harvest.

When dealing with AquaCrop performance according to soil class, the analysis of model simulations permitted us to draw partial conclusions only. The analysis of the model outputs for the AGB and SWC showed an acceptable performance in simulating these two variables across all soil classes. For runoff and CC, the best results were observed with Vertisols and Cambisols, respectively. For ET_a, for which we had measurements on Vertisols only, no conclusion can be drawn regarding AquaCrop performance according to soil class.

When dealing with linear regressions on validation for both crop types and soil classes, the t test provided p values larger than 5% for most cases (e.g., AGB, CC, SWC), which indicated that AquaCrop performances could be considered satisfactory. For some crop/soil combinations, the t test provided p values lower than 5% (e.g., ET_a, R, SWC), although the offset remained relatively low (e.g., ET_a and SWC offset for oats and Cambisols, respectively).

5.7. Main outcomes

To our knowledge, the present work is the first study using AquaCrop for faba bean and oats in a semiarid Mediterranean climate. According to the results we obtained, AquaCrop can acceptably simulate the functioning of these two crops by using crop parameters available in the literature. Additionally, AquaCrop simulations are acceptable for various combinations of soils and crops across contrasted hydroclimatic years.

Although there were gaps in database on which the current study relied, it was rich enough to draw several lessons. According to the results we obtained, the model performance was closely related to the formalism used for simulations. AquaCrop showed good performance in simulating biomass and soil water content for all crops, on the basis of parameterizations and forcing (1) that were as adequate as possible for the crops and soils to be studied, and (2) that were in line with literature recommendations. The performance of the model was moderate for the simulation of CC, with a possible delay in senescence for most of the crops we addressed. The model showed acceptable performance in simulating ET_a, although it was delicate to conclude according to the dataset size (2 years - plots).

Runoff was poorly simulated at both the beginning and end of the crop cycle because of shrinkage cracks for clay soils. Soil cracking is a complex phenomenon that is very difficult to include in numerical modelling, especially in simplified models. Runoff simulations were acceptable for the other stages of the crop cycle when the cracks were closed. Despite this, the simulations were acceptable to simulate the dynamics of soil water content and crop variables (AGB), as shown in Figs. 4-5-9-10 and Tabs 5-6-10-11, which was ascribed to the moderate influence of runoff on the soil water balance. However, in the perspective of agro-hydrological studies that require the consideration of lateral fluxes between the different components of the cultivated landscape (Van Loo and Verstraeten, 2021), the runoff modelling by AquaCrop was no longer acceptable for our study site, and it will be necessary to consider a more realistic runoff-infiltration partitioning model.

6. Conclusion

For some soil/crop combinations that have been little studied to date, AquaCrop can acceptably simulate their functioning in terms of vegetation growth and water consumption, as well as in terms of soil water balance, by using parameters available in the literature. Additionally, AquaCrop can simultaneously simulate several variables in an acceptable manner, namely, aboveground biomass, evapotranspiration, and soil water content. We highlight some limitations of AquaCrop in terms of vegetation cover and runoff in relation to delayed senescence and disregard of swelling soils, respectively.

The results of the current study are in good agreement with those reported in the literature, knowing that the previous studies mainly addressed flat terrains. Our study also showed that AquaCrop was able to acceptably simulate crop dynamics and water fluxes for contrasted hydroclimatic years, with a slight dependence on soil class and a significant dependence on crop type, including large differences from one variable to another.

Our results open the path for further use of AquaCrop in the Mediterranean context, on which we focused, with forthcoming efforts on water availability and water productivity in relation to plot hydrological connectivities within hilly terrains.

Acknowledgements

The first author benefited from funding provided by the Tunisian Ministry of Higher Education and Scientific Research (MESRS) and the French National Research Institute for Sustainable Development (IRD) to carry out her Ph.D. research. The current study is part of the ALTOS project in the framework of the PRIMA program, with financial contributions from France and Tunisia. The authors would like to thank (1) the Environmental Research Observatory OMERE (http://www.obs-omere.org), which policy drives the availability of the data used in the current study, and Damien Raclot, (2) Guillaume Coulouma (INRAE/UMR LISAH) for the help and expertise provided in soil science, and (3) Marie Weiss (INRAE/UMR EMMAH) for the exchanges about CAN-EYE software.

References

Abrha, B., Delbecque, N., Raes, D., Tsegay, A., Todorovic, M., Heng, L., Vanutrecht, E., Geerts, S., Garcia-Vila, M., Deckers, S., 2012. Sowing strategies for barley (HORDEUM VULGARE L.) based on modelled yield response to water with AQUACROP. Experimental Agriculture 48, 252–271.

Ahmadi, S.H., Mosallaeepour, E., Kamgar-Haghighi, A.A., Sepaskhah, A.R., 2015. Modeling Maize Yield and Soil Water Content with AquaCrop Under Full and Deficit Irrigation Managements. Water Resource Management 29, 2837–2853.

Alaya, I., Masmoudi, M.M., Jacob, F., Ben Mechlia, N., 2019. Up-scaling of crop productivity estimations using the AquaCrop model and GIS-based operations. Arabian Journal of Geosciences 12, 419.

Allen, R.G., PEREIRA, L.S., RAES, D., SMITH, M. (Eds.), 1998. Crop evapotranspiration: guidelines for computing crop water requirements, reprography. ed, FAO irrigation and drainage paper. Food and Agriculture Organization of the United Nations, Rome.

Andarzian, B., Bannayan, M., Steduto, P., Mazraeh, H., Barati, M.E., Barati, M.A., Rahnama, A., 2011. Validation and testing of the AquaCrop model under full and deficit irrigated wheat production in Iran. Agricultural Water Management 100, 1–8.

Araya, A., Habtu, S., Hadgu, K.M., Kebede, A., Dejene, T., 2010. Test of AquaCrop model in simulating biomass and yield of water deficient and irrigated barley (Hordeum vulgare). Agricultural Water Management 97, 1838–1846.

Bhattacharya, A., 2019. Chapter 3 - Water-Use Efficiency Under Changing Climatic Conditions, Changing Climate and Resource Use Efficiency in Plants (A. Bhattacharya, Ed), Academic Press, Pages 111-180, ISBN 9780128162095.

Besbes, B., Fournaraki, C., Tavolaro, F.M., Koutsovoulou, K., Leroy, G., Hoffmann, I., 2016. Chapitre 6 - Diversité des ressources végétales et animales. Presses de Sciences Po.

Bird, D.N., Benabdallah, S., Gouda, N., Hummel, F., Koeberl, J., La Jeunesse, I., Meyer, S., Prettenthaler, F., Soddu, A., Woess-Gallasch, S., 2016. Modelling climate change impacts on and adaptation strategies for agriculture in Sardinia and Tunisia using AquaCrop and value-at-risk. Science of The Total Environment, Special Issue on Climate Change, Water and Security in the Mediterranean 543, 1019–1027.

Boudhina, N., Masmoudi, M.M., Alaya, I., Jacob, F., Ben Mechlia, N., 2019. Use of AquaCrop model for estimating crop evapotranspiration and biomass production in hilly topography. Arabian Journal of Geosciences 12, 259.

Boudhina, N., Masmoudi, M.M., Ben Mechlia, N., Zitouna, R., Mekki, I., Prévot, L., Jacob, F., 2017a. Evapotranspiration of Wheat in a Hilly Topography: Results from Measurements Using a Set of Eddy Covariance Stations, in: Ouessar, M., Gabriels, D., Tsunekawa, A., Evett, S. (Eds.), Water and Land Security in Drylands: Response to Climate Change. Springer International Publishing, Cham, pp. 67–76.

Boudhina, N., Masmoudi, M.M., Jacob, F., Prévot, L., Zitouna, R., Mekki, I., Kallel, A., Ksibi, M., Ben Dhia, H., Khélifi, N., 2017b. Measuring Crop Evapotranspiration Over Hilly Areas, in: Recent Advances in Environmental Science from the Euro-Mediterranean and Surrounding Regions. Springer International Publishing, pp. 909–911.

Boudhina, N., Zitouna-Chebbi, R., Mekki, I., Jacob, F., Ben Mechlia, N., Masmoudi, M., Prévot, L., 2018. Evaluating four gap-filling methods for eddy covariance measurements of evapotranspiration over hilly crop fields. Geoscientific Instrumentation, Methods and Data Systems 7, 151–167.

Brisson, N., Gary, C., Justes, E., Roche, R., Mary, B., Ripoche, D., Zimmer, D., Sierra, J., Bertuzzi, P., Burger, P., Bussière, F., Cabidoche, Y.M., Cellier, P., Debaeke, P., Gaudillère, J.P., Hénault, C., Maraux, F., Seguin, B., Sinoquet, H., 2003. An overview of the crop model STICS. European Journal of Agronomy, Modelling Cropping Systems: Science, Software and Applications 18, 309–332.

Brun, M., Blanc, P., Otto, H., 2016. Chapitre 1 - Perspective globale des ressources naturelles. Presses de Sciences Po.

Cassel, D.K., Nielsen, D.R., 1986. Field Capacity and Available Water Capacity, in: Klute, A. (Ed.), SSSA Book Series. Soil Science Society of America, American Society of Agronomy, Madison, WI, USA, pp. 901–926.

Constantin, J., Willaume, M., Murgue, C., Lacroix, B., Therond, O., 2015. The soil-crop models STICS and AqYield predict yield and soil water content for irrigated crops equally well with limited data. Agricultural and Forest Meteorology 206, 55–68.

Cusicanqui, J., Dillen, K., Garcia, M., Geerts, S., Raes, D., Mathijs, E., 2013. Economic assessment at farm level of the implementation of deficit irrigation for quinoa production in the Southern Bolivian Altiplano. Spanish Journal of Agricultural Research 11, 894.

de Wit, A., Boogaard, H., Fumagalli, D., Janssen, S., Knapen, R., van Kraalingen, D., Supit, I., van der Wijngaart, R., van Diepen, K., 2019. 25 years of the WOFOST cropping systems model. Agricultural Systems 168, 154–167.

Deb, P., Shrestha, S., Babel, M.S., 2015. Forecasting climate change impacts and evaluation of adaptation options for maize cropping in the hilly terrain of Himalayas: Sikkim, India. Theoretical and Applied Climatology 121, 649–667.

El Mokh, F., Vila-Garcia, Nagaz, K., Masmoudi, M.M., Ben Mechlia, N., Fereres, E., 2017.

Calibration of AquaCrop Salinity Stress Parameters for Barley Under Different Irrigation Regimes in a Dry Environment, in: Water and Land Security in Drylands; Response to Climate Change.

Er-Raki, S., Bouras, E., Rodriguez, J.C., Watts, C.J., Lizarraga-Celaya, C., Chehbouni, A., 2021. Parameterization of the AquaCrop model for simulating table grapes growth and water productivity in an arid region of Mexico. Agricultural Water Management 245, 106585.

García-López, J., Lorite, I., García-Ruiz, R., Domínguez, J., 2014. Evaluation of three simulation approaches for assessing yield of rainfed sunflower in a Mediterranean environment for climate change impact modelling. Climatic Change 124, 147–162.

García-Vila, M., Fereres, E., 2012. Combining the simulation crop model AquaCrop with an economic model for the optimization of irrigation management at farm level. European Journal of Agronomy 36, 21–31.

Geerts, S., Raes, D., Garcia, M., Taboada, C., Miranda, R., Cusicanqui, J., Mhizha, T., Vacher, J., 2009. Modeling the potential for closing quinoa yield gaps under varying water availability in the Bolivian Altiplano. Agricultural Water Management 96, 1652–1658.

Han, C., Zhang, B., Chen, H., Wei, Z., Liu, Y., 2019. Spatially distributed crop model based on remote sensing. Agricultural Water Management 218, 165–173.

Inoubli, N., 2016. Ruissellement et érosion hydrique en milieu méditerranéen vertique : approche expérimentale et modélisation (thèse de doctorat). Montpellier SupAgro ; Institut national agronomique de Tunisie.

Inoubli, N., Raclot, D., Mekki, I., Moussa, R., Le Bissonnais, Y., 2017. A Spatiotemporal Multiscale Analysis of Runoff and Erosion in a Mediterranean Marly Catchment. Vadose Zone Journal 16:1-12.

International Assessment of Agricultural Knowledge, Science and Technology for Development Executive Summary of the Synthesis Report, 2008. International Assessment of Agricultural Knowledge, Science and Technology for Development.

Jacob, F., Olioso, A., Weiss, M., Baret, F., Hautecoeur, O., 2002. Mapping short-wave albedo of agricultural surfaces using airborne PolDER data. Remote Sensing of Environment 80, 36–46.

Jamieson, P.D., Porter, J.R., Wilson, D.R., 1991. A test of the computer simulation model ARCWHEAT1 on wheat crops grown in New Zealand. Field Crops Research 27, 337–350.

Jonckheere, I., Fleck, S., Nackaerts, K., Muys, B., Coppin, P., Weiss, M., & Baret, F., 2004. Review of methods for in situ leaf area index determination: Part I. Theories, sensors and hemispherical photography. Agricultural and Forest Meteorology, 121(1-2), 19-35.

Jones, J.W., Antle, J.M., Basso, B., Boote, K.J., Conant, R.T., Foster, I., Godfray, H.C.J., Herrero, M., Howitt, R.E., Janssen, S., Keating, B.A., Munoz-Carpena, R., Porter, C.H., Rosenzweig, C., Wheeler, T.R., 2017. Brief history of agricultural systems modeling. Agricultural Systems 155, 240–254.

Jones, J.W., Hoogenboom, G., Porter, C.H., Boote, K.J., Batchelor, W.D., Hunt, L.A., Wilkens, P.W., Singh, U., Gijsman, A.J., Ritchie, J.T., 2003. The DSSAT cropping system model. European Journal of Agronomy, Modelling Cropping Systems: Science, Software and Applications 18, 235–265.

Kanda, E., Mabhaudhi, T., Senzanje, A., 2018. Coupling hydrological and crop models for improved agricultural water management – A review. Bulgarian Journal of Agricultural Science 23, 380.

Katerji, N., Campi, P., Mastrorilli, M., 2013. Productivity, evapotranspiration, and water use efficiency of corn and tomato crops simulated by AquaCrop under contrasting water stress conditions in the Mediterranean region. Agricultural Water Management 130, 14–26.

Katerji, N., Rana, G., 2006. Modelling evapotranspiration of six irrigated crops under Mediterranean climate conditions. Agricultural and Forest Meteorology 138, 142–155.

Keating, B.A., Carberry, P.S., Hammer, G.L., Probert, M.E., Robertson, M.J., Holzworth, D., Huth, N.I., Hargreaves, J.N.G., Meinke, H., Hochman, Z., McLean, G., Verburg, K., Snow, V., Dimes, J.P., Silburn, M., Wang, E., Brown, S., Bristow, K.L., Asseng, S., Chapman, S., McCown, R.L., Freebairn, D.M., Smith, C.J., 2003. An overview of APSIM, a model designed for farming systems simulation. European Journal of Agronomy, Modelling Cropping Systems: Science, Software and Applications 18, 267–288.

Kustas, W.P., Humes, K.S., Norman, J.M., Moran, M.S., 1996. Single- and Dual-Source Modeling of Surface Energy Fluxes with Radiometric Surface Temperature. Journal of Applied Meteorology and Climatology 35, 110–121.

Leuning, R., van Gorsel, E., Massman, W.J., Isaac, P.R., 2012. Reflections on the surface energy imbalance problem. Agricultural and Forest Meteorology 156, 65–74.

Lovelli, S., Perniola, M., Ferrara, A., Di Tommaso, T., 2007. Yield response factor to water (Ky) and water use efficiency of Carthamus tinctorius L. and Solanum melongena L. Agricultural Water Management 92, 73–80.

Lu, Y., Chibarabada, T.P., McCabe, M.F., De Lannoy, G.J.M., Sheffield, J., 2021. Global sensitivity analysis of crop yield and transpiration from the FAO-AquaCrop model for dryland environments. Field Crops Research 269, 108182.

Masasi, B., Taghvaeian, S., Gowda, P.H., Warren, J., Marek, G., 2019. Simulating Soil Water

Content, Evapotranspiration, and Yield of Variably Irrigated Grain Sorghum Using AquaCrop. Journal of the American Water Resources Association 55(4), 976–993.

Mekki, I., 2003. Analyse et modélisation de la variabilité des flux hydriques à l’échelle d’un bassin versant cultivé alimentant un lac collinaire du domaine semi-aride méditerranéen (Oued Kamech, Cap Bon, Tunisie) (Thèse de doctorat). Montpellier 2.

Mekki, I., Albergel, J., Ben Mechlia, N., Voltz, M., 2006. Assessment of overland flow variation and blue water production in a farmed semi-arid water harvesting catchment. Physics and Chemistry of the Earth, Parts A/B/C 31, 1048–1061.

Mekki, I., Bailly, J.S., Jacob, F., Chebbi, H., Ajmi, T., Blanca, Y., Zairi, A., Biarnès, A., 2018. Impact of farmland fragmentation on rainfed crop allocation in Mediterranean landscapes: A case study of the Lebna watershed in Cap Bon, Tunisia. Land Use Policy 75, 772–783.

Mkhabela, M.S., Bullock, P.R., 2012. Performance of the FAO AquaCrop model for wheat grain yield and soil moisture simulation in Western Canada. Agricultural Water Management 110, 16–24.

Molénat, J., Raclot, D., Zitouna, R., Andrieux, P., Coulouma, G., Feurer, D., Grünberger, O., Lamachère, J.M., Bailly, J.S., Belotti, J.L., Ben Azzez, K., Ben Mechlia, N., Ben Younès Louati, M., Biarnès, A., Blanca, Y., Carrière, D., Chaabane, H., Dagès, C., Debabria, A., Dubreuil, A., Fabre, J.C., Fages, D., Floure, C., Garnier, F., Geniez, C., Gomez, C., Hamdi, R., Huttel, O., Jacob, F., Jenhaoui, Z., Lagacherie, P., Le Bissonnais, Y., Louati, R., Louchart, X., Mekki, I., Moussa, R., Negro, S., Pépin, Y., Prévot, L., Samouelian, A., Seidel, J.L., Trotoux, G., Troiano, S., Vinatier, F., Zante, P., Zrelli, J., Albergel, J., Voltz, M., 2018. OMERE: A Long-Term Observatory of Soil and Water Resources, in Interaction with Agricultural and Land Management in Mediterranean Hilly Catchments. Vadose Zone Journal 17: 1-18 180086.

Montes, C., Lhomme, J.-P., Demarty, J., Prévot, L., Jacob, F., 2014. A three-source SVAT modeling of evaporation: Application to the seasonal dynamics of a grassed vineyard. Agricultural and Forest Meteorology 191, 64–80.

Moriasi, D.N., Arnold, J.G., Liew, M.W., Bingner, R.L., Harmel, R.D., Veith, T.L., 2007. Model Evaluation Guidelines for Systematic Quantification of Accuracy in Watershed Simulations. Transactions of the ASABE 50, 885–900.

Moriasi, D.N., Gitau, M.W., Pai, N., Daggupati, D., 2015. Hydrologic and Water Quality Models: Performance Measures and Evaluation Criteria. Transactions of the ASABE 58, 1763–1785.

Mubvuma, Michael.T., Ogola, J.B.O., Mhizha, T., 2021. AquaCrop model calibration and validation for chickpea (Cicer arietinum) in Southern Africa. Cogent Food & Agriculture 7, 1898135.

Muluneh, A., 2020. Impact of climate change on soil water balance, maize production, and potential adaptation measures in the Rift Valley drylands of Ethiopia. Journal of Arid Environments 179, 104195.

Norouzi, M., Ayoubi, S., Jalalian, A., Khademi, H., Dehghani, A.A., 2010. Predicting rainfed wheat quality and quantity by artificial neural network using terrain and soil characteristics. Acta Agriculturae Scandinavica, Section B — Soil & Plant Science 60, 341–352.

Nouri, H., Stokvis, B., Chavoshi Borujeni, S., Galindo, A., Brugnach, M., Blatchford, M.L., Alaghmand, S., Hoekstra, A.Y., 2020. Reduce blue water scarcity and increase nutritional and economic water productivity through changing the cropping pattern in a catchment. Journal of Hydrology 588, 125086.

Nyakudya, I.W., Stroosnijder, L., 2014. Effect of rooting depth, plant density and planting date on maize (Zea mays L.) yield and water use efficiency in semi-arid Zimbabwe: Modelling with AquaCrop. Agricultural Water Management 146, 280–296.

Nyathi, M.K., van Halsema, G.E., Annandale, J.G., Struik, P.C., 2018. Calibration and validation of the AquaCrop model for repeatedly harvested leafy vegetables grown under different irrigation regimes. Agricultural Water Management 208, 107–119.

Pereira, L.S., Paredes, P., Rodrigues, G.C., Neves, M., 2015. Modeling malt barley water use and evapotranspiration partitioning in two contrasting rainfall years. Assessing AquaCrop and SIMDualKc models. Agricultural Water Management 159, 239–254.

Qin, W., Chi, B., Oenema, O., 2013. Long-Term Monitoring of Rainfed Wheat Yield and Soil Water at the Loess Plateau Reveals Low Water Use Efficiency. PLOS ONE 8, e78828.

Raes, D., Steduto, P., Hsiao, T.C., Fereres, E., 2009. AquaCrop -The FAO Crop Model to Simulate Yield Response to Water: II. Main Algorithms and Software Description. Agronomy Journal 101, 438–447.

Raoufi, R.S., Soufizadeh, S., 2020. Simulation of the impacts of climate change on phenology, growth, and yield of various rice genotypes in humid sub-tropical environments using AquaCrop-Rice. International Journal of Biometeorology 64, 1657–1673.

Rashid, M.A., Jabloun, M., Andersen, M.N., Zhang, X., Olesen, J.E., 2019. Climate change is expected to increase yield and water use efficiency of wheat in the North China Plain. Agricultural Water Management 222, 193–203.

Reichstein, M., Falge, E., Baldocchi, D., Papale, D., Aubinet, M., Berbigier, P., Bernhofer, C., Buchmann, N., Gilmanov, T., Granier, A., Grünwald, T., Havránková, K., Ilvesniemi, H., Janous, D., Knohl, A., Laurila, T., Lohila, A., Loustau, D., Matteucci, G., Meyers, T., Miglietta, F., Ourcival, J.-M., Pumpanen, J., Rambal, S., Rotenberg, E., Sanz, M., Tenhunen, J., Seufert, G., Vaccari, F., Vesala, T., Yakir, D., Valentini, R., 2005. On the separation of net ecosystem exchange into assimilation and ecosystem respiration: review and improved algorithm. Global Change Biology 11, 1424–1439.

Robinson, D.A., Campbell, C.S., Hopmans, J.W., Hornbuckle, B.K., Jones, S.B., Knight, R., Ogden, F., Selker, J., Wendroth, O., 2008. Soil Moisture Measurement for Ecological and Hydrological Watershed-Scale Observatories: A Review. Vadose Zone Journal 7, 358–389.

Ruben, R., Pender, J., 2004. Rural diversity and heterogeneity in less-favoured areas: the quest for policy targeting. Food Policy 29, 303–320.

Salman, M., García-Vila, M., Fereres, E., Raes, D., Steduto, P., 2021. The AquaCrop model–Enhancing crop water productivity: Ten years of development, dissemination and implementation 2009–2019 (Vol. 47). Food & Agriculture Organisation.

Sandhu, R., Irmak, S., 2019. Performance of AquaCrop model in simulating maize growth, yield, and evapotranspiration under rainfed, limited and full irrigation. Agricultural Water Management 223, 105687.

Sghaier, N., Masmoudi, M.M., Ben Mechlia, N., 2014. Paramétrage du modèle AquaCrop pour la simulation de la culture du blé dur. Revue des Régions Arides, 35, 1351-1360.

Shrestha, S., Deb, P., Bui, T.T.T., 2016. Adaptation strategies for rice cultivation under climate change in Central Vietnam. In: Climate Change Impacts and Adaptation in Water Resources and Water Use Sectors. Springer Water. Springer, Cham 21, 15–37.

Silvestro, P.C., Pignatti, S., Pascucci, S., Yang, H., Li, Z., Guijun, Y., Huang, W., Casa, R., 2017. Estimating Wheat Yield in China at the Field and District Scale from the Assimilation of Satellite Data into the AquaCrop and Simple Algorithm for Yield (SAFY) Models. Remote Sensing 9, 509.

Sreelash, K., Buis, S., Sekhar, M., Ruiz, L., Kumar Tomer, S., Guérif, M., 2017. Estimation of available water capacity components of two-layered soils using crop model inversion: Effect of crop type and water regime. Journal of Hydrology 546, 166–178.

Steduto, P., Hsiao, T.C., Raes, D., Fereres, E., 2009. AquaCrop-The FAO Crop Model to Simulate Yield Response to Water: I. Concepts and Underlying Principles. Agronomy Journal 101, 426–437.

Stöckle, C.O., Donatelli, M., Nelson, R., 2003. CropSyst, a cropping systems simulation model. European Journal of Agronomy, Modelling Cropping Systems: Science, Software and Applications 18, 289–307.

Susha Lekshmi, S.U., Singh, D.N., Shojaei Baghini, M., 2014. A critical review of soil moisture measurement. Measurement 54, 92–105.

Tanyeri-Abur, A., 2015. Food Security in the Southern Mediterranean/North Africa, in: Vastola, A. (Ed.), The Sustainability of Agro-Food and Natural Resource Systems in the Mediterranean Basin. Springer International Publishing, Cham, pp. 3–14.

Todorovic, M., Albrizio, R., Zivotic, L., Saab, M.-T.A., Stöckle, C., Steduto, P., 2009. Assessment of AquaCrop, CropSyst, and WOFOST Models in the Simulation of Sunflower Growth under Different Water Regimes. Agronomy Journal 101, 509–521.

Toumi, J., Er-Raki, S., Ezzahar, J., Khabba, S., Jarlan, L., Chehbouni, A., 2016. Performance assessment of AquaCrop model for estimating evapotranspiration, soil water content and grain yield of winter wheat in Tensift Al Haouz (Morocco): Application to irrigation management. Agricultural Water Management 163, 219–235.

Tribouillois, H., Constantin, J., Willaume, M., Brut, A., Ceschia, E., Tallec, T., Beaudoin, N., Therond, O., 2018. Predicting water balance of wheat and crop rotations with a simple model: AqYield. Agricultural and Forest Meteorology 262, 412–422.

Van Loo, M., Verstraeten, G., 2021. A Spatially Explicit Crop Yield Model to Simulate Agricultural Productivity for Past Societies under Changing Environmental Conditions. Water 13, 2023.

Vanuytrecht, E., Raes, D., Willems, P., 2014. Global sensitivity analysis of yield output from the water productivity model. Environmental Modelling & Software 51, 323–332.

Walker, J.P., Willgoose, G.R., Kalma, J.D., 2004. In situ measurement of soil moisture: a comparison of techniques. Journal of Hydrology 293, 85–99.

Wani, S.P., Rockström, J., Oweis, T.Y., 2009. Rainfed Agriculture: Unlocking the Potential. CAB International, Wallingford, UK.

Weiss, M., Jacob, F., Duveiller, G., 2020. Remote sensing for agricultural applications: A meta-review. Remote Sensing of Environment, 236, 111402.

Williams, J.R., Jones, C.A., Dyke, P.T., 1984. A modelling approach to determining the relationship between erosion and soil productivity [EPIC, Erosion-Productivity Impact Calculator, mathematical models]. Transactions of the ASAE [American Society of Agricultural Engineers] (USA).

Wolka, K., Biazin, B., Martinsen, V., Mulder, J., 2021. Soil and water conservation management on hill slopes in southwest Ethiopia. II. Modeling effects of soil bunds on surface runoff and maize yield using AquaCrop. Journal of Environmental Management 296, 113187.

Xing, H., Xu, X., Li, Z., Chen, Y., Feng, H., Yang, G., Chen, Z., 2017. Global sensitivity analysis of the AquaCrop model for winter wheat under different water treatments based on the extended Fourier amplitude sensitivity test. Journal of Integrative Agriculture 16, 2444–2458.

Yang, J.M., Yang, J.Y., Liu, S., Hoogenboom, G., 2014. An evaluation of the statistical methods for testing the performance of crop models with observed data. Agricultural Systems 127, 81–89.

Yuan, M., Zhang, L., Gou, F., Su, Z., Spiertz, J.H.J., van der Werf, W., 2013. Assessment of crop growth and water productivity for five C3 species in semi-arid Inner Mongolia. Agricultural Water Management 122, 28–38.

Zeleke, K.T., 2019. AquaCrop Calibration and Validation for Faba Bean (Vicia faba L.) under Different Agronomic Managements. Agronomy 9, 320.

Zitouna-Chebbi, R., Prévot, L., Chakhar, A., Marniche-Ben Abdallah, M., Jacob, F., 2018. Observing Actual Evapotranspiration from Flux Tower Eddy Covariance Measurements within a Hilly Watershed: Case Study of the Kamech Site, Cap Bon Peninsula, Tunisia. Atmosphere 9, 68.

Zitouna-Chebbi, R., Prévot, L., Jacob, F., Mougou, R., Voltz, M., 2012. Assessing the consistency of eddy covariance measurements under conditions of sloping topography within a hilly agricultural catchment. Agricultural and Forest Meteorology 164, 123–135.

Zitouna-Chebbi, R., Prévot, L., Jacob, F., Voltz, M., 2015. Accounting for vegetation height and wind direction to correct eddy covariance measurements of energy fluxes over hilly crop fields. Journal of Geophysical Research: Atmospheres 120, 4920–4936.

Supplementary materials - Section 1: materials and methods - soil parameters

Different approaches are proposed in the literature to determine soil moisture at wilting point (HWP) and at field capacity (HFC), including (1) pedotransfer functions (e.g., Saxton and Rawls, 2006) based on the texture of different soil horizons, (2) direct laboratory measurements from soil samples (Cassel and Nielsen, 1986) and (3) the agroclimatic method which determines HFC and HWP from soil moisture time series throughout the crop growth cycle (Sreelash et al., 2017).

According to expert knowledge about the soil conditions within our study site (Revaillot et al., 2021), the pedotransfer functions are not suitable for the Kamech soils, since the latter are typified by large instability due to poor silt structure. Therefore, we determine HWP and HFC using the laboratory method and the agroclimatic method, and we compared the resulting estimates in order to choose the most reliable ones.

For all plots, we had laboratory measurements of HFC and HWP carried out either on the plots or on neighbouring plots, along with soil moisture data. For the agroclimatic method proposed by Sreelash et al. (2017), HFC corresponds to the maximum soil moisture value without considering measurements after rainfalls or irrigation events, and HWP corresponds to the 5th percentile of the minimum soil moisture measured throughout the crop growth cycle. To determine HFC and HWP by the agroclimatic method, we used all soil moisture data available for each of the eight plots, beyond the datasets used for AquaCrop evaluation. This led to include additional soil moisture data from 2002 on plot P5 and P8, from 2001 and plot P6 and P9, and from 2006 on plot A. All the soil moisture measurements we considered were collected using the same protocol described in the Section 3.3.6 of the article. For HFC, we assumed that a rainfall accumulation lower than 10 mm does not have a large influence, and we therefore excluded all measurements for which a rainfall accumulation larger than 10 mm was recorded in the previous 48 hours. For HWP, we take the 5th percentile of the minimum value measured throughout the crop growth cycle.

Table SP1 presents, for each plot, HWP and HFC estimates by laboratory measurements (Lab), and by the agroclimatic method (AC), as well as the relative difference Δ calculated as:

$$\Delta = \frac{AC - Lab}{Lab} \qquad \text{(Equation SP1)}$$

where AC (respectively Lab) represents the HWP or HFC estimates by the agroclimatic method (respectively the laboratory method).

Table SP1 shows that HWP estimates from the agroclimatic method underestimated those from the laboratory method, with values of relative difference Δ between -26% and -18%, apart from plot D (32%). For HFC, the differences between the two methods were small, with values of relative difference Δ between -3% and 10%, apart from plot P8 (24%). In this case, HFC estimates from the agroclimatic method overestimated those from the laboratory method, apart from plot P6.

Table SP1. Comparison between soil moisture at wilting point (HWP) and soil moisture at field capacity (HFC) estimates by the laboratory measurements (Lab) and the agroclimatic method (AC) methods.

	HWP			**HFC**		
	AC (m^3/m^3)	**lab (m^3/m^3)**	**Δ (%)**	**AC (m^3/m^3)**	**lab (m^3/m^3)**	**Δ (%)**
P5	0.23	0.31	-26	0.45	0.41	10
P6	0.21	0.27	-22	0.35	0.36	-3
P7	0.23	0.31	-26	0.44	0.41	7
P8	0.19	0.24	-21	0.46	0.37	24
P9	0.25	0.33	-24	0.47	0.45	4
A	0.28	0.34	-18	0.44	0.43	2
B	0.26	0.34	-24	0.44	0.43	2
D	0.23	0.34	-32	0.44	0.43	2

Fig. SP1 displays the times series of soil moisture measurements, as well as the HFC and HWP estimates from (1) the laboratory measurements (HWP-lab and HFC-lab), and (2) the agroclimatic method (HWP-AC and HFC-AC) for each of all plots. Fig. SP1 shows that, apart from plot A, the soil moisture measurements before the harvest dates reach lower levels than the HWP estimates from the laboratory measurements.

As a result, we selected the estimates from the agroclimatic method for all plots apart from plot A. For plot A, the differences between estimates from both methods were very low (10% relative, comparable to measurement errors), and we selected the estimates from laboratory measurements that were collected in the framework of the OMERE observatory.

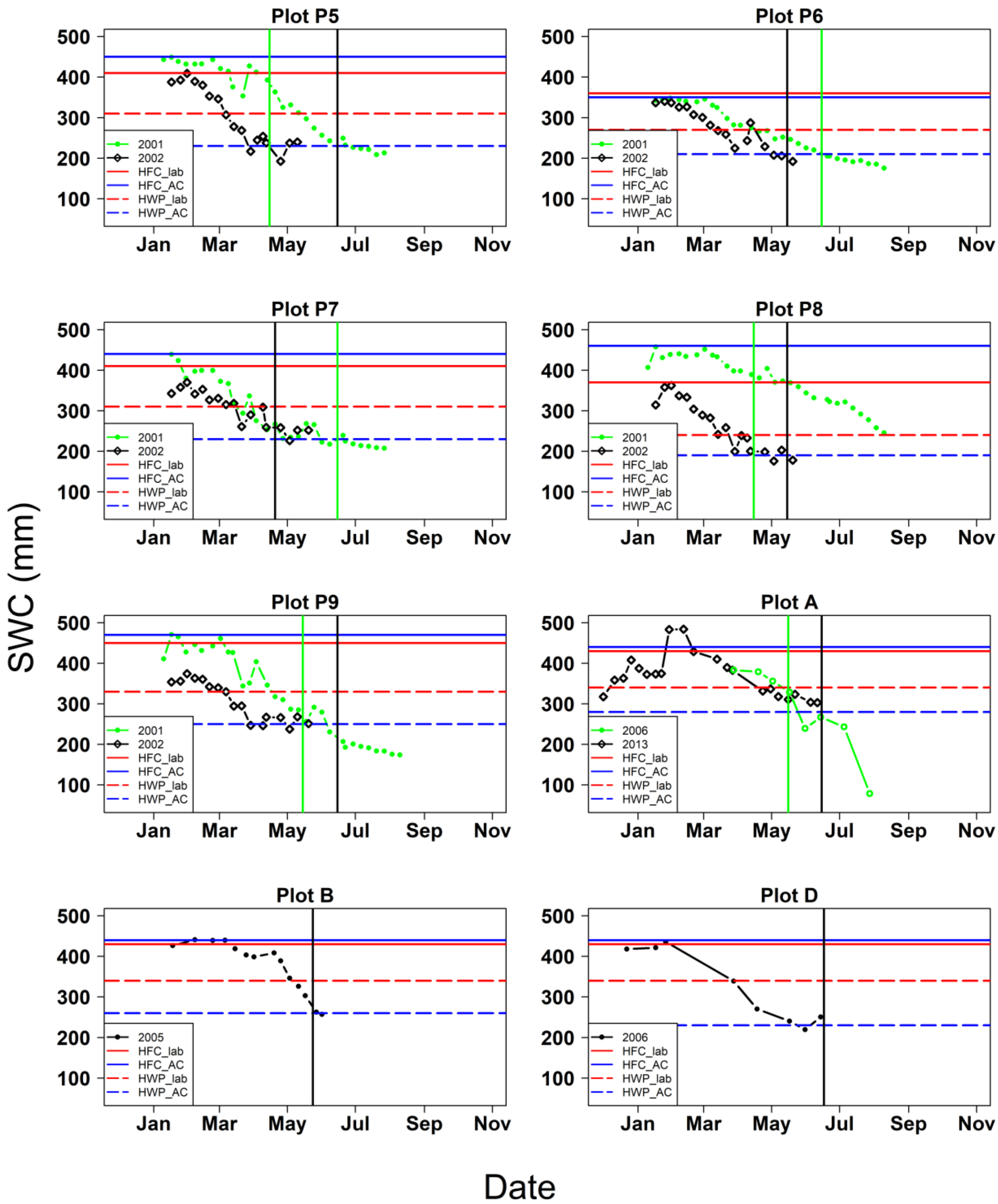

Fig. SP1. Time series of soil moisture data (dotted lines) for each of the eight plots. The horizontal lines indicate the soil moisture at wilting point (HWP) and soil moisture at field capacity (HFC) estimates from the laboratory measurements (Lab) (red lines) and agroclimatic method (AC) (blue lines) methods. The vertical lines indicate the harvest dates.

Supplementary materials - Section 2: Materials and methods – Vegetation

When dealing with growth cycle of cereals (wheat, barley, oats), we could use leaf area index (LAI) measurements performed with planimeters. In order to validate the AquaCrop simulations of canopy cover (CC), we used Equation SP2 to convert planimetry-based LAI data into CC, considering that this equation had been used in many studies (Araya et al., 2010; Abrha et al., 2012; Yuan et al., 2013; Pereira et al., 2015; Zeleke, 2019):

$$CC = 1 - e^{(-k \times LAI)} \qquad \text{(Equation SP2)}$$

The coefficient k is an extinction coefficient related to the interception of light by crop canopy cover (Jeuffroy and Ney, 1997; Pereira et al., 2015). It varies according to crop and variety. Different values of k have been proposed in literature for a given crop. For example, the proposed values for barley are k = 0.5 (Pereira et al., 2015), k = 0.48 (Belhouchette et al., 2008) and k = 0.65 (Abrha et al., 2012). For wheat, (Jin et al., 2014) proposed a k value of 0.65.

To determine a k value that was suitable to our conditions, we used hemispherical photos that permitted to simultaneously estimate LAI and CC. These photos were collected between 2018 and 2020 thanks to a camera equipped with a fisheye objective. Within each plot, between 10 and 15 photos were collected in a random manner. Table SP2 summarises the number of plots and measurements available per crop.

Table SP2. Number of plots and hemispherical photos available for each crop, to be used for determining the value of coefficient k in Equation SP2.

Crop	Years	Plot number	Measurements number
Wheat	2018 - 2019 - 2020	8	42
Barley	2019 - 2020	2	10
Oats	2020	1	4

The hemispherical photos were treated with the CAN-EYE software (Weiss et al., 2008) to derive first gap fraction, and then LAI and CC. CAN-EYE permitted to distinguish two types of LAI, namely (1) effective LAI that accounts for leaf aggregation, and (2) true LAI that corresponds to actual leaf surface. The different LAI estimates proposed by CAN-EYE are discussed in Weiss et al. (2008).

- On the one hand, planimetry is a direct and destructive technique for determining leaf area index of any crop canopy. It permits the calculation of actual LAI from direct area measurements.

- On the other hand, hemispherical photography is an indirect, non-destructive technique that permits a significant spatiotemporal sampling of crop canopy within field and throughout the crop growth cycle. It includes other plant green elements such as stems, which corresponds to Plant Area Index (PAI) rather than LAI.
- The goal here was to convert planimetric measurements of LAI into CC estimates by using Equation SP2. When estimating LAI from hemispherical photos, it was necessary to select the CAN-EYE method that provided LAI estimates as close as possible to the planimetric method. According to Weiss et al (2008), the true LAI calculated by CAN-EYE is the closest to the planimetric LAI, although the relationship between true LAI measured by CAN-EYE and planimetric LAI depends on crop and phenological stage (Demarez et al., 2008; Fang et al., 2018). Therefore, we choose true LAI for equation SP2.

For the present study, we decided to set a single k value for cereals (wheat, barley and oats), equal to 0.57 (R2 = 0.95; RMSE = 0.05). Indeed, the coefficient of variation between the different k values across cereal crops was about 15%, thus comparable to the measurement error (Weiss et al., 2008). Moreover, the three cereal crops we considered were straw cereals with similar leaf geometry that induces similar radiative transfer processes within the canopy.

Supplementary materials - Section 3. Results –canopy cover (CC)

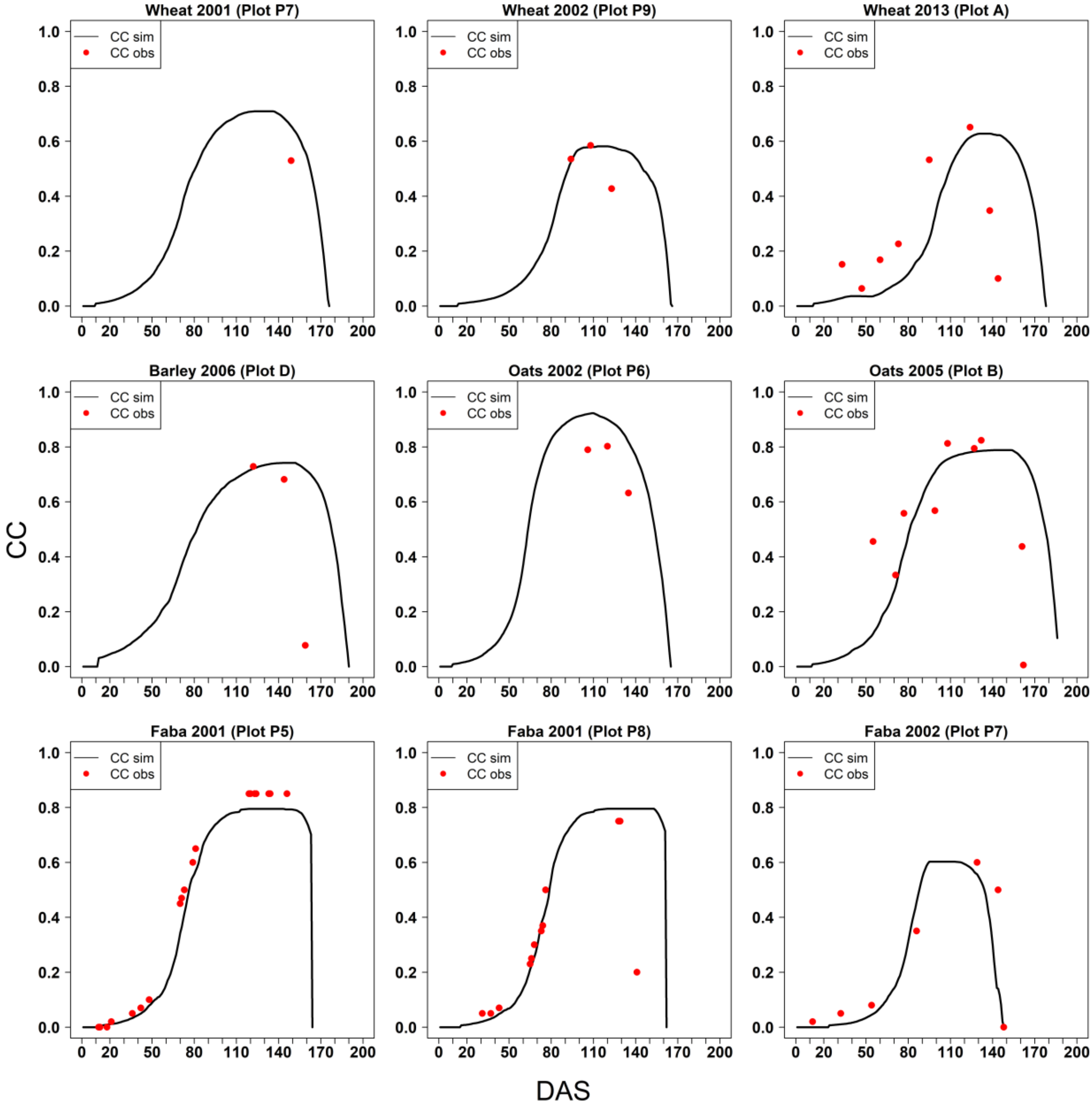

Fig. SP2. Temporal evolution of canopy cover (CC) for each dataset when available. The red points correspond to the ground-based observations, and the black curves correspond to the AquaCrop simulations. DAS stands for Day after Sowing.

Supplementary materials - Section 4. Results - aboveground biomass (AGB)

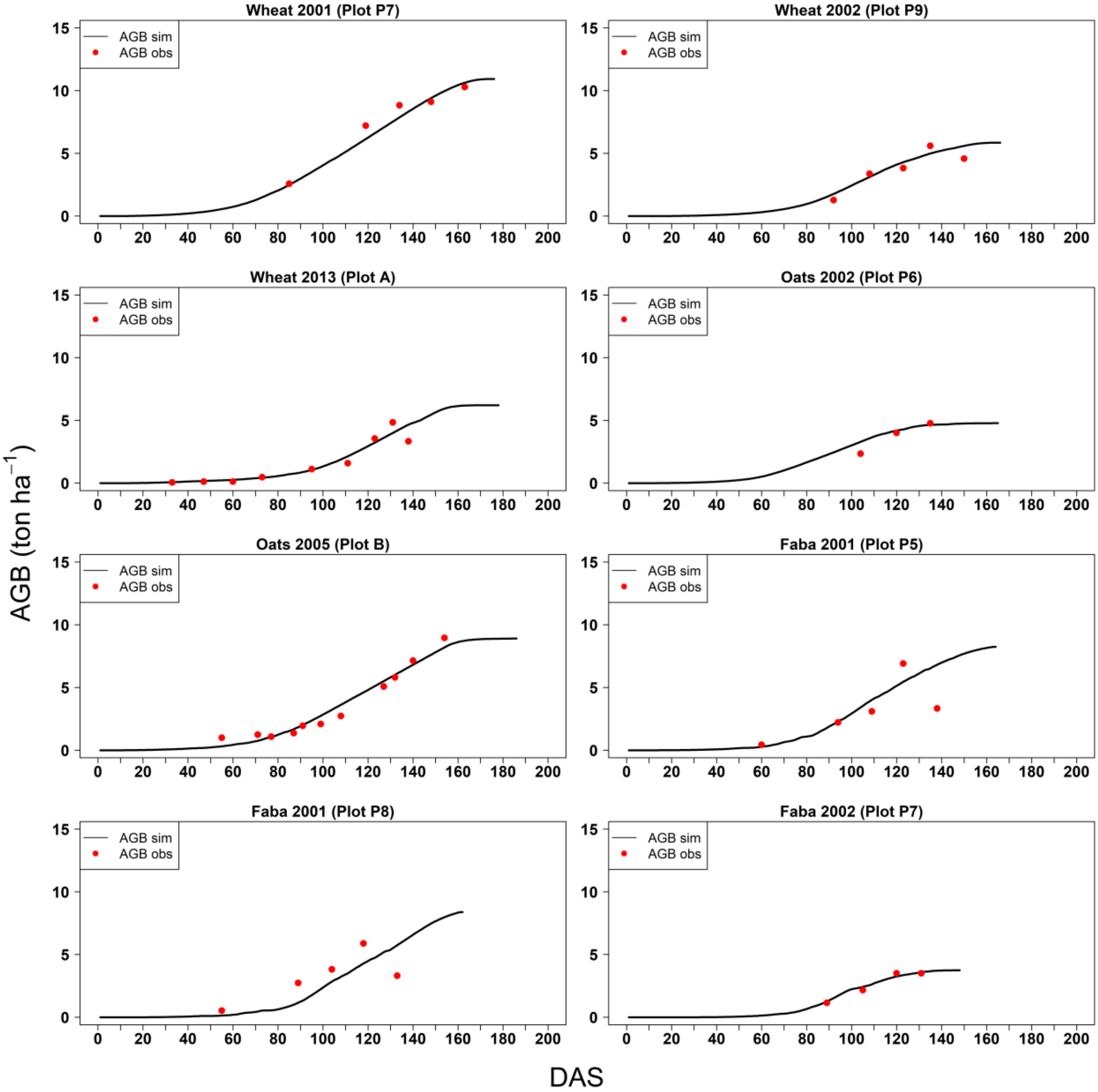

Fig. SP3. Temporal evolution of Aboveground biomass **(**AGB) for each dataset when available. The red points correspond to observations and the black curve corresponds to AquaCrop simulations. DAS stands for Day after Sowing.

Supplementary materials - Section 5. Results - actual evapotranspiration (ETa)

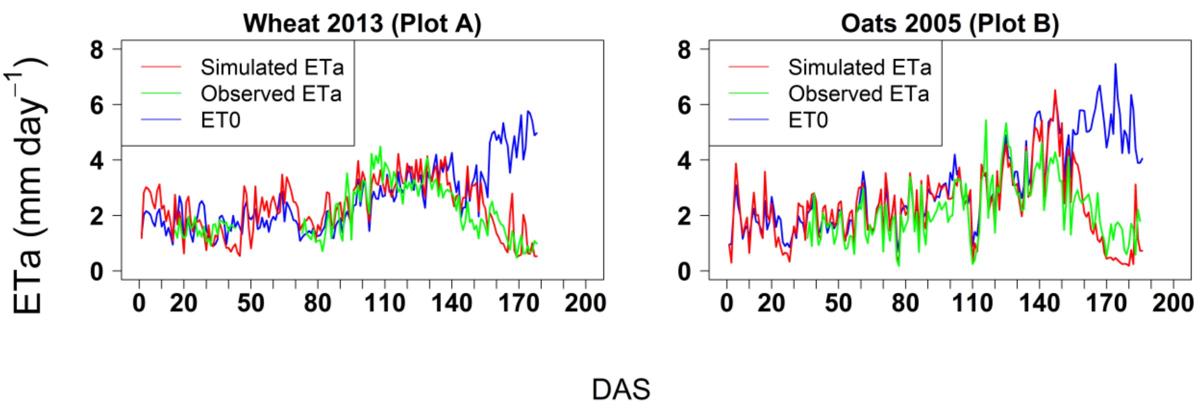

Fig. SP4. Temporal evolution of actual evapotranspiration (ETa) for each dataset when available. The red curve corresponds to ETa simulated by AquaCrop, the green curve corresponds to ETa measured in-situ by eddy covariance and the blue curve corresponds to reference evapotranspiration ET0. DAS stands for Day after Sowing.

Supplementary materials - Section 6. Results – runoff (R)

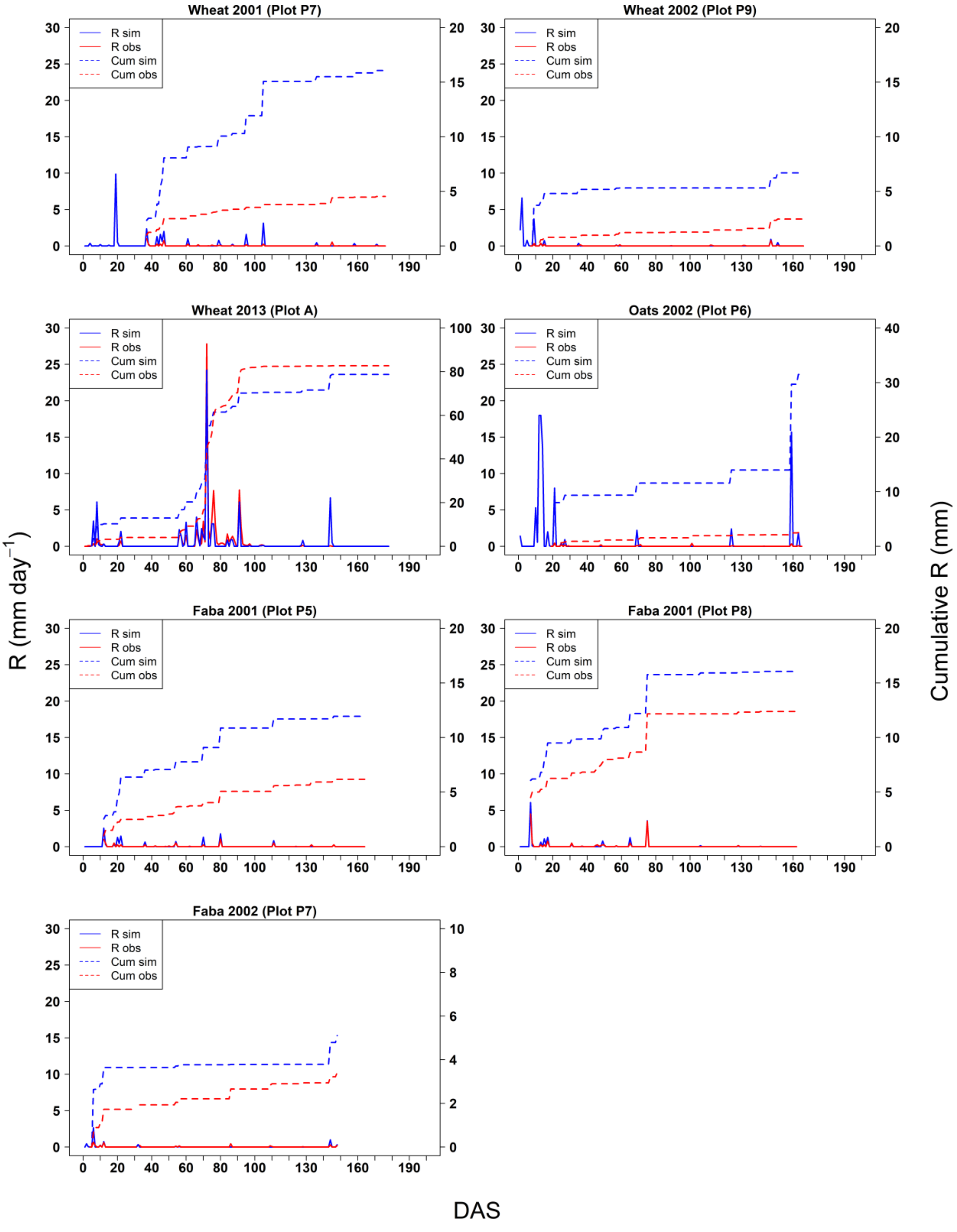

Fig. SP5. Temporal evolution of runoff (R) for each dataset when available. The solid lines represent the temporal evolution of R. The dashed lines represent R accumulation. The blue colour indicates the simulations and the red colour indicates the observations. DAS stands for Day after Sowing. Y-Scales are chosen for both reading and intercomparing.

Supplementary materials - Section 7. Results – soil water content (SWC)

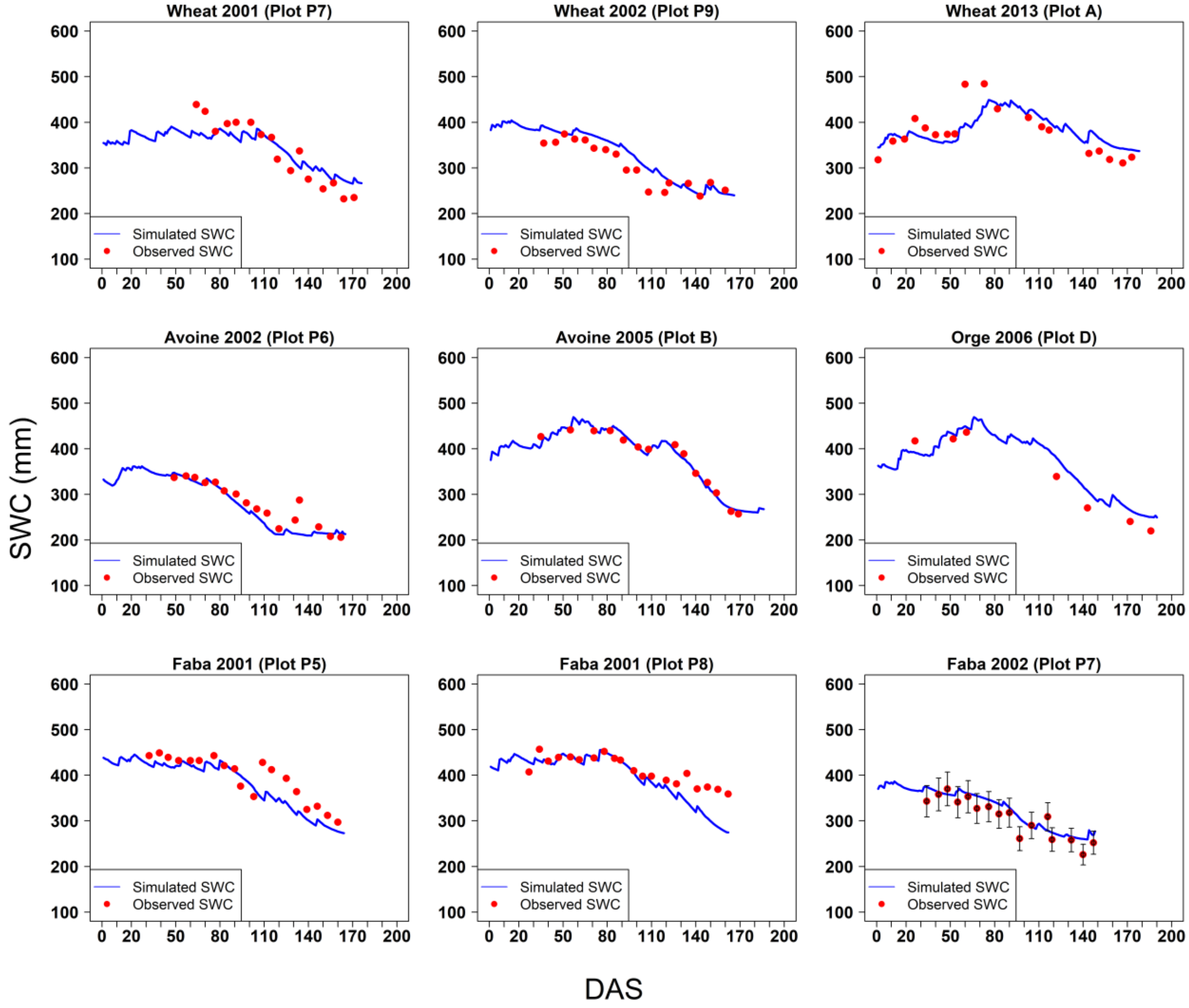

Fig. SP6. Temporal evolution of soil water content (SWC) for each dataset. The red points correspond to SWC observations, and the blue curves correspond to the AquaCrop simulations. DAS stands for Day after Sowing.

References

Abrha, B., Delbecque, N., Raes, D., Tsegay, A., Todorovic, M., Heng, L., Vanutrecht, E., Geerts, S., Garcia-Vila, M., Deckers, S., 2012. Sowing strategies for barley (HORDEUM VULGARE L.) based on modelled yield response to water with AQUACROP. Experimental Agriculture 48, 252–271.

Araya, A., Habtu, S., Hadgu, K.M., Kebede, A., Dejene, T., 2010. Test of AquaCrop model in simulating biomass and yield of water deficient and irrigated barley (Hordeum vulgare). Agricultural Water Management 97, 1838–1846.

Belhouchette, H., Breaudeau, E., Hachicha, M., Donatelli, M., Mohtar, R.H., Wery, J., 2008. Integrating spatial soil organization data with a regional agricultural management simulation model: a case study in Northern Tunisia. Transactions of the ASABE 51, 1099–1109.

Cassel, D.K., Nielsen, D.R., 1986. Field Capacity and Available Water Capacity, in: Klute, A. (Ed.), SSSA Book Series. Soil Science Society of America, American Society of Agronomy, Madison, WI, USA, pp. 901–926.

Demarez, V., Duthoit, S., Baret, F., Weiss, M., Dedieu, G., 2008. Estimation of leaf area and clumping indexes of crops with hemispherical photographs. Agricultural and Forest Meteorology 148, 644–655.

Fang, H., Ye, Y., Liu, W., Wei, S., Ma, L., 2018. Continuous estimation of canopy leaf area index (LAI) and clumping index over broadleaf crop fields: An investigation of the PASTIS-57 instrument and smartphone applications. Agricultural and Forest Meteorology 253–254, 48–61.

Jeuffroy, M.-H., Ney, B., 1997. Crop physiology and productivity. Field Crops Research, Improvement of Grain Legumes 53, 3–16.

Jin, X., Feng, H., Zhu, X., Li, Z., Song, S., Song, X., Yang, G., Xu, X., Guo, W., 2014. Assessment of the AquaCrop Model for Use in Simulation of Irrigated Winter Wheat Canopy Cover, Biomass, and Grain Yield in the North China Plain. PLOS ONE 9, e86938.

Pereira, L.S., Paredes, P., Rodrigues, G.C., Neves, M., 2015. Modeling malt barley water use and evapotranspiration partitioning in two contrasting rainfall years. Assessing AquaCrop and SIMDualKc models. Agricultural Water Management 159, 239–254.

Revaillot, S., Pouget, C., Alvarez, G., Fontaine, S., 2021. Mesurer la capacité de rétention en eau d'un sol par centrifugation : une méthode fiable, facile et rapide à mettre en œuvre dans un laboratoire (Les Cahiers des techniques de l'INRA). INRA.

Saxton, K.E., Rawls, W.J., 2006. Soil Water Characteristic Estimates by Texture and Organic Matter for Hydrologic Solutions. Soil Science Society of America Journal 70, 1569–1578.

Sreelash, K., Buis, S., Sekhar, M., Ruiz, L., Kumar Tomer, S., Guérif, M., 2017. Estimation of available water capacity components of two-layered soils using crop model inversion: Effect of crop type and water regime. Journal of Hydrology 546, 166–178.

Weiss, M., Baret, F., de Solan, B., Demarez, V., Bertrand, N., 2008. CAN-EYE, logiciel de traitement d'images pour l'estimation de l'indice foliaire. Le cahier des techniques de l'INRA. Pratique et outils de mesure des rayonnements naturels 159–166.

Yuan, M., Zhang, L., Gou, F., Su, Z., Spiertz, J.H.J., van der Werf, W., 2013. Assessment of crop growth and water productivity for five C3 species in semi-arid Inner Mongolia. Agricultural Water Management 122, 28–38.

Zeleke, K.T., 2019. AquaCrop Calibration and Validation for Faba Bean (Vicia faba L.) under Different Agronomic Managements. Agronomy 9, 320.